

Supplementary Materials for

HIV-1 vaccine design through minimizing envelope metastability

Linling He, Sonu Kumar, Joel D. Allen, Deli Huang, Xiaohu Lin, Colin J. Mann, Karen L. Saye-Francisco, Jeffrey Copps, Anita Sarkar, Gabrielle S. Blizard, Gabriel Ozorowski, Devin Sok, Max Crispin, Andrew B. Ward, David Nemazee, Dennis R. Burton, Ian A. Wilson*, Jiang Zhu*

*Corresponding author. Email: wilson@scripps.edu (I.A.W.); jiang@scripps.edu (J.Z.)

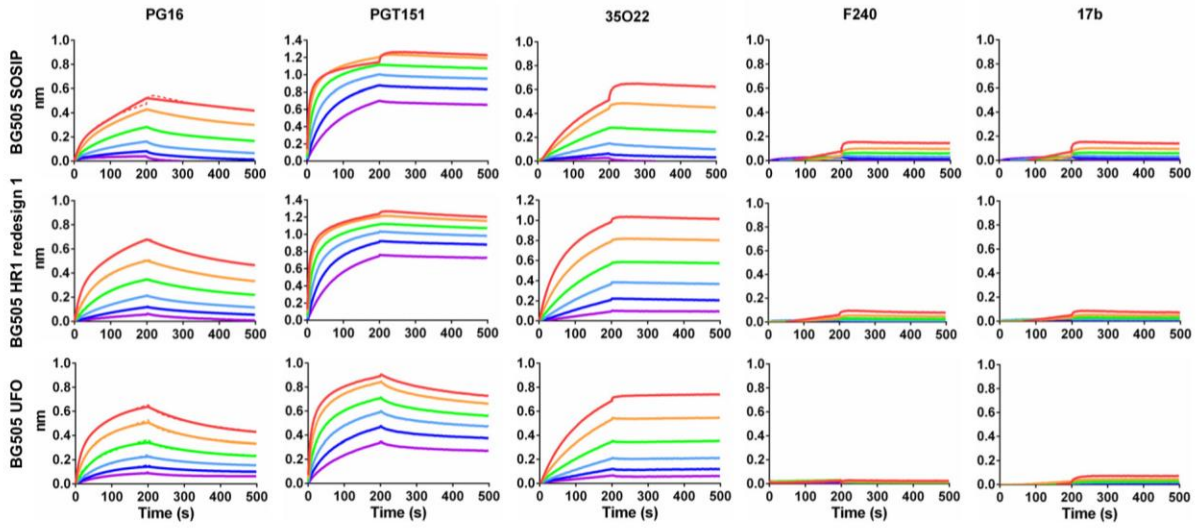
Published 21 November 2018, *Sci. Adv.* **4**, eaau6769 (2018)

DOI: 10.1126/sciadv.aau6769

This PDF file includes:

- Fig. S1. Effect of expression system on antigenicity and glycosylation of BG505 Env trimers.
- Fig. S2. Biochemical and biophysical characterization of diverse Env trimers.
- Fig. S3. Structural characterization of diverse UFO-BG trimers.
- Fig. S4. Antigenic profiles of UFO and UFO-BG trimers derived from 10 strains of five subtypes assessed against a panel of 11 bNAbs, 8 non-NAbs, and CD4-Ig.
- Fig. S5. Evolutionary root of metastability and design of UFO-C trimers containing a database-derived ancestral gp41_{ECTO}.
- Fig. S6. Characterization of gp41_{ECTO}-stabilized trimer-presenting nanoparticles.
- Fig. S7. B cell activation and in vivo evaluation of gp41_{ECTO}-stabilized trimers and nanoparticles.
- Table S1. X-ray data collection and refinement statistics.

A



B

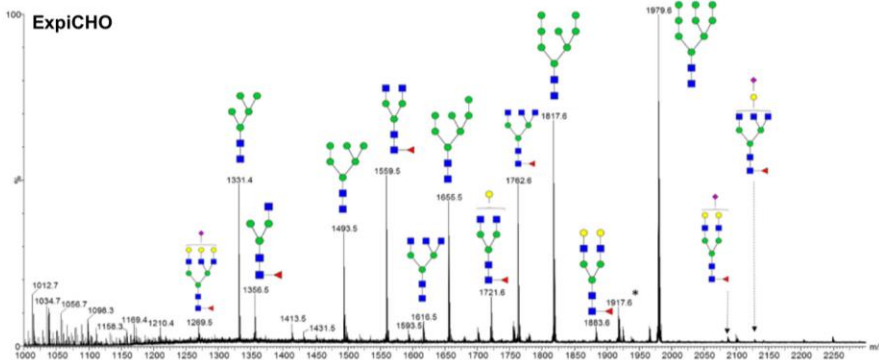
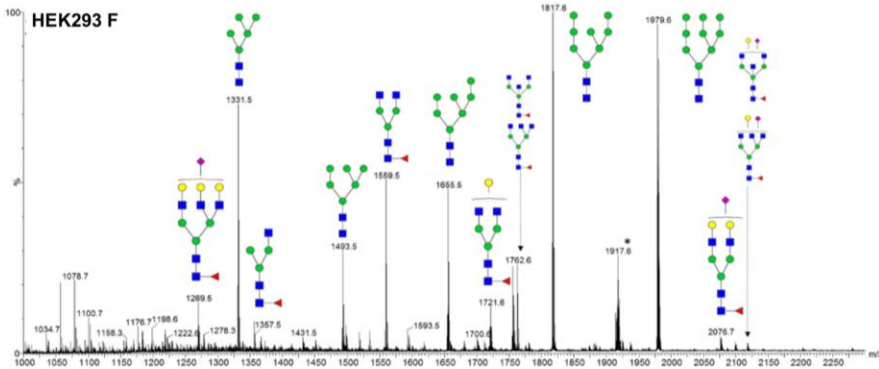
HEK293 F

TOTAL OLIGOMANNOSE CONTENT	
Man5-9	56.42%
Man5	5.99%
Man6	3.24%
Man7	5.52%
Man8	15.48%
Man9	26.19%

ExpiCHO

TOTAL OLIGOMANNOSE CONTENT	
Man5-9	64.49%
Man5	6.17%
Man6	5.12%
Man7	4.15%
Man8	12.81%
Man9	29.69%

C



Glycan Key:

Fucose



Galactose



Glucose



Mannose



Sialic acid



N-acetyl
glucosamine



D

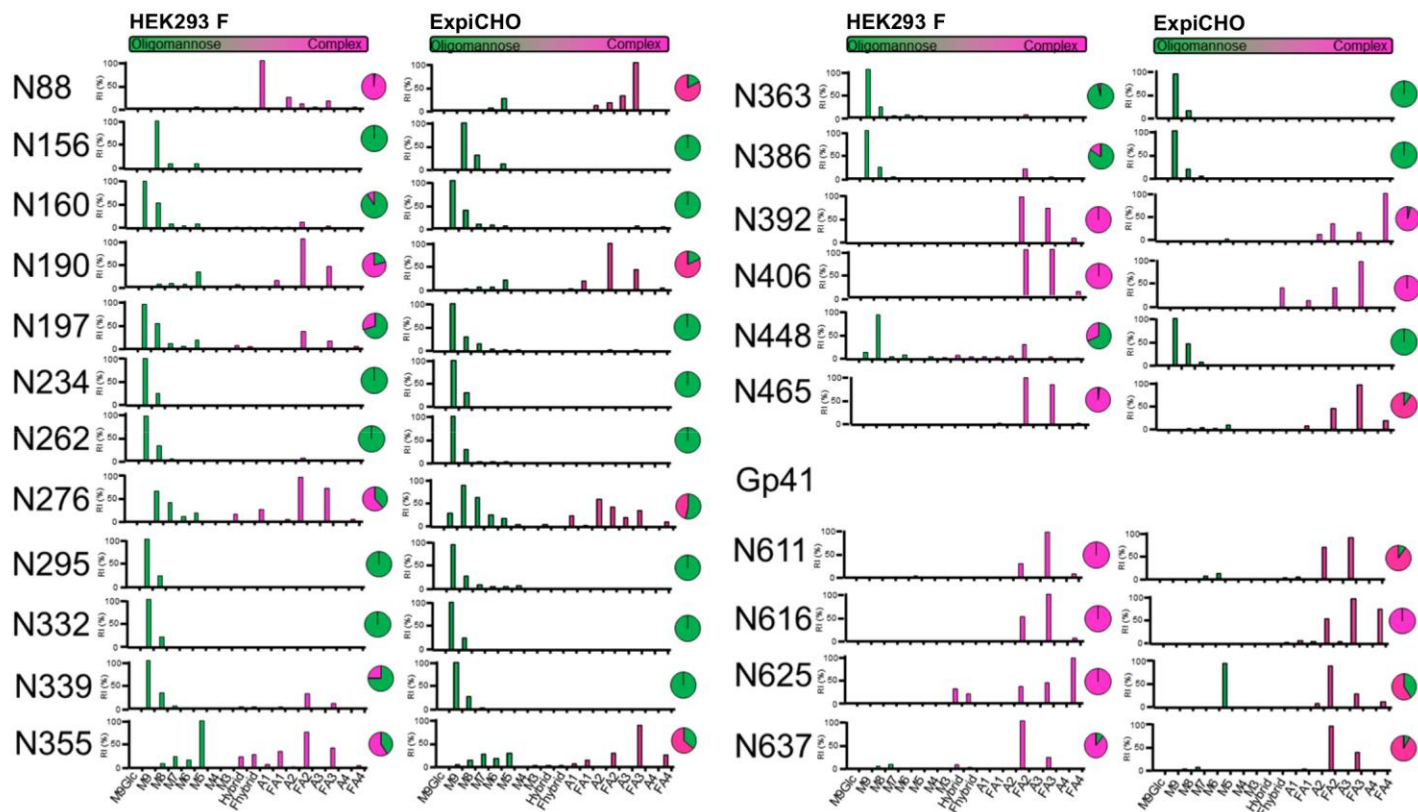
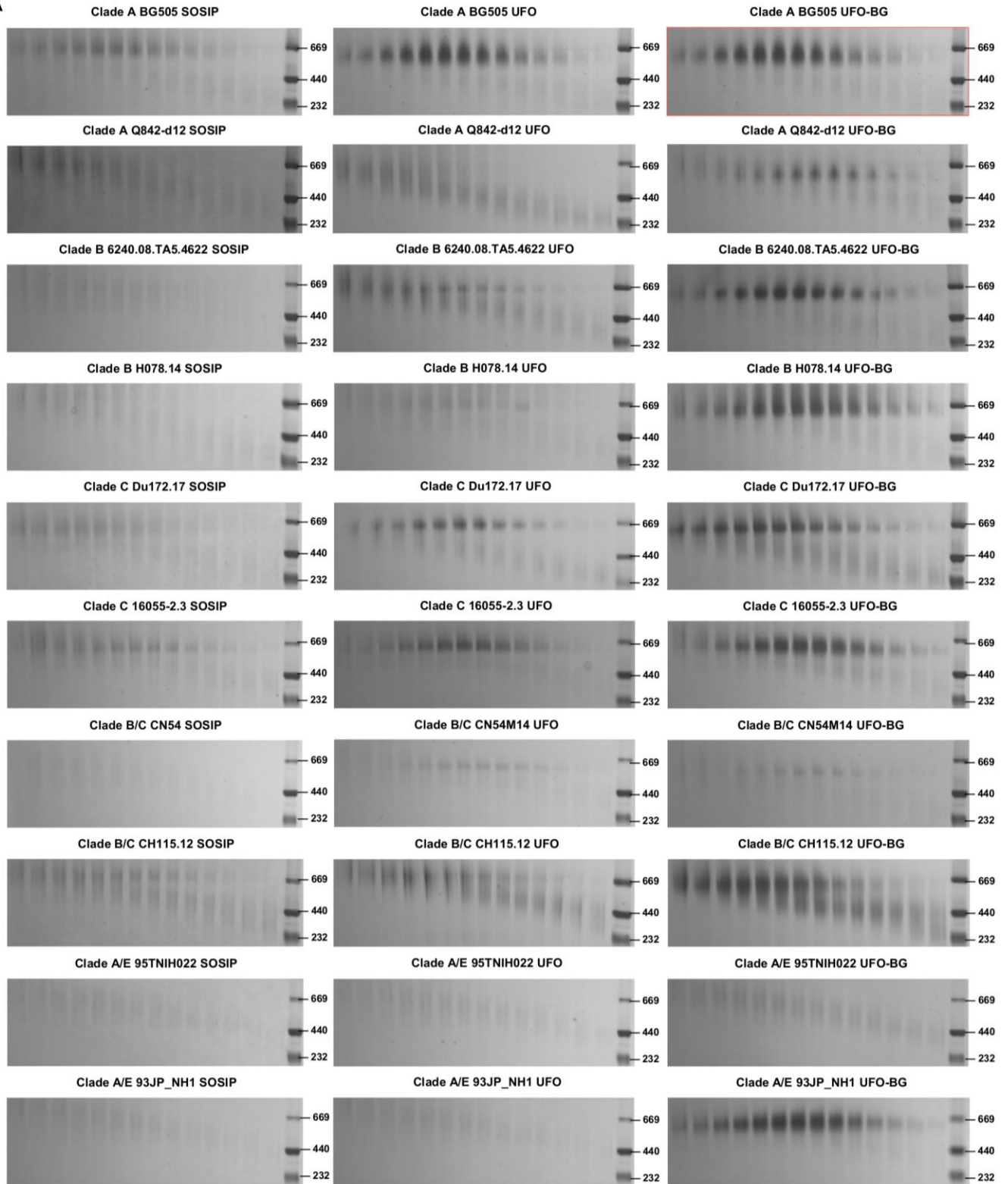
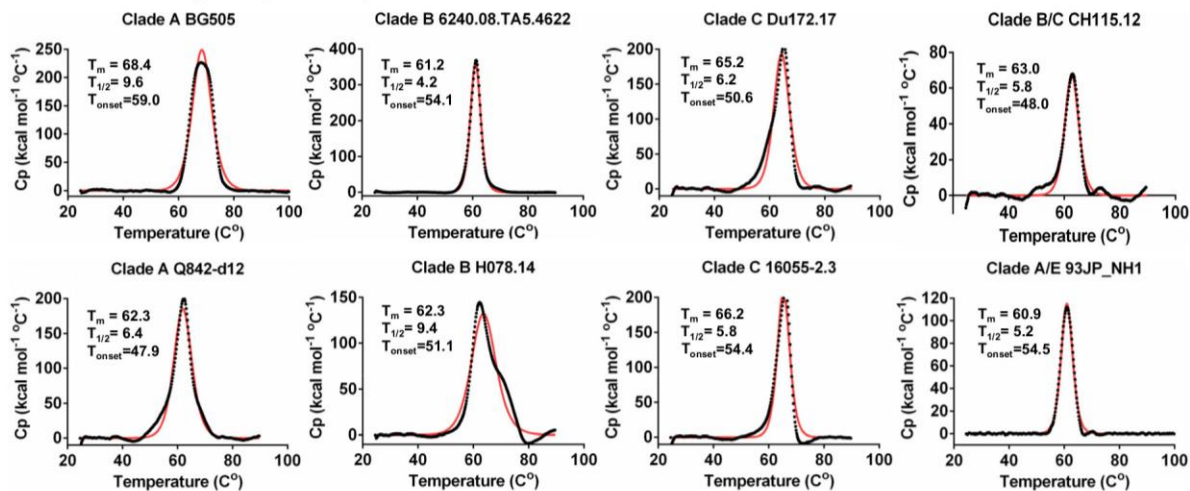


Fig. S1. Effect of expression system on antigenicity and glycosylation of BG505 Env trimers. (A) Additional antigenic profiles for SOSIP, HR1-redesigned, and UFO trimers derived from clade A BG505. Sensorgrams were obtained from an Octet RED96 instrument using a titration series of six trimer concentrations (200-6.25 nM by 2-fold dilution). (B) Total oligomannose content for a BG505 trimer produced in HEK293 F and ExpiCHO cells. (C) Ion mobility mass spectrometry analysis of a BG505 trimer produced in HEK293 F and ExpiCHO cells. Mobility-extracted singly charged negative-ion electrospray spectra are shown for N-linked glycans on gp140. (D) Quantitative site-specific N-glycosylation of a BG505 trimer produced in HEK293 F and ExpiCHO cells, with relative quantification shown for N-glycosylation sites on both gp120 and gp41_{ECTO}. The gp140 construct used in (B)-(D) is the HR1 redesign 1 (or termed gp140.664.R1), which is the immediate predecessor of the UFO design.

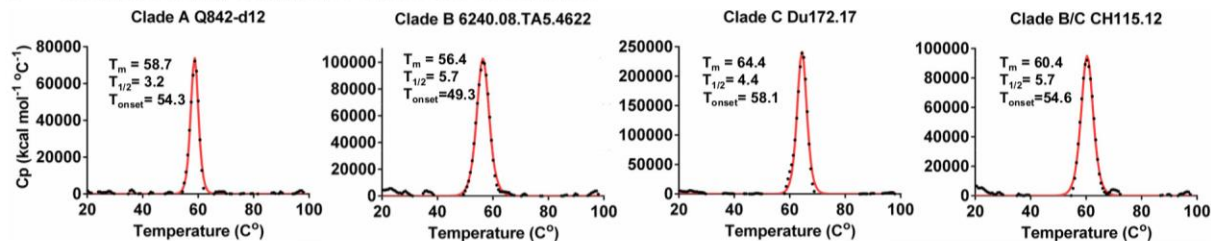
A



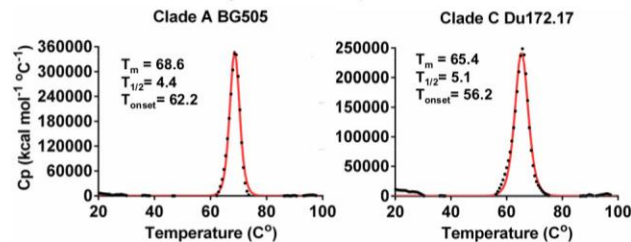
B Thermal stability of ExpiCHO-expressed UFO-BG trimers



C Thermal stability of ExpiCHO-expressed UFO trimers



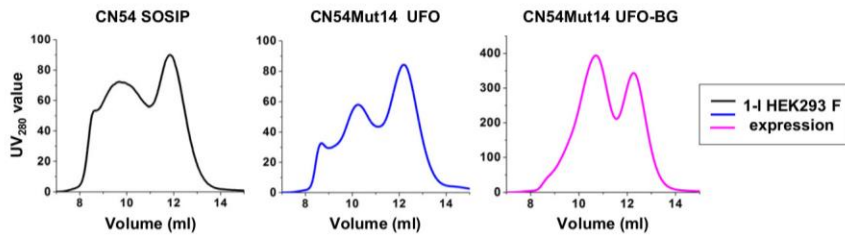
D Thermal stability of 293 F-expressed UFO/UFO-BG trimers



E

>CN54Mut14 (the generic UFO design)

MDAMKRGLCCVLLLCGAVFVSPSQEIHARFRRGARVGNLWVTVVYGVVPVWkdAeTTLFCASDAKAYDTEkHNVWATHACVPADPNPQEMVLENVT
 ENFNMWKNEMVNMQQtDVISLWDQSLKPCVKLTPLCVTLLECRNVSSNSNDTYHETHEHSMKEMKNCNCFNATTVLRDRKQTVYALFYRLDIVPLTK
 KNYSENSSEYRLINCNTSAITQACPVTDFDPIPIHYCTPAGYAILKCNDFINFGTGPCHNVSTVQCTHGKIPVSTQLLLNGSLAEGEIIIRSE
 NLTNNVKTIIIVHLNQSVEIVCTRPNGNTRKSIRIRGPGQTFYATGDIIGDIRQAHcNISEDKWNELQRVSKKLAEHVFNQNTIKFASSGGDLEVT
 THSFNCgGEFFYCNTSGLFNGAYTPNGTKNSSSIIITPCRIKQIINMWQzVRGRAMYAPPKIGNIzCvSNITGLLLVRDGGTEPNDETFRPGGG
 DMRNNWRSELYKYKVVVEIKPLGVAPTzCKRRRVVEGGGGSGGGSAVGIGAVFLGFLGVAGSTMGAASmPLTVQARnLLSGSGSGSTVWGIKQ
 LQTRVLAIERYLzDQQLLGIWGCSGKLIcCtNVPWNSSWSNKSQKEIWDNMTWMQWdKEISNYTNTVYRLLSESNQQRNEKDLLALD



F

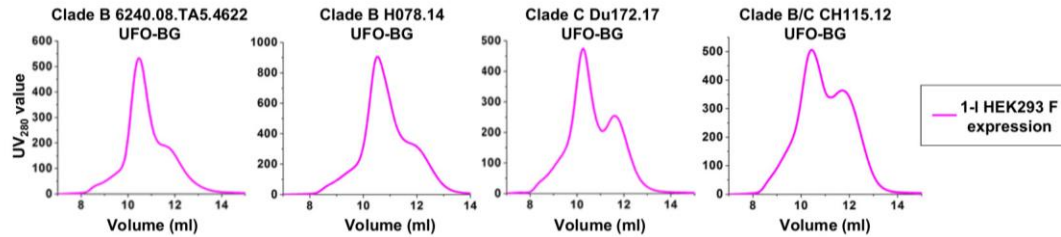
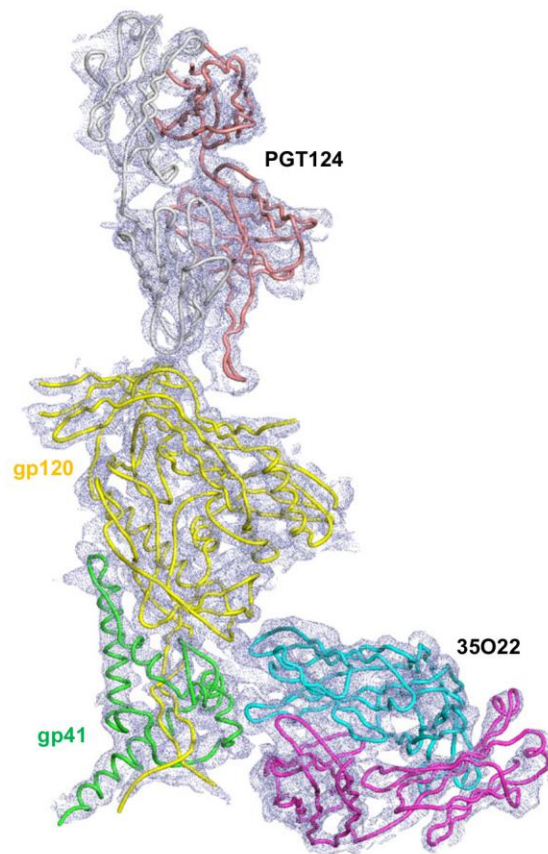


Fig. S2. Biochemical and biophysical characterization of diverse Env trimers. (A) BN-PAGE of ExpiCHO-expressed, GNL-purified Env proteins for SOSIP, UFO, and UFO-BG trimers derived from ten strains of five subtypes (A, B, C, B/C, and A/E) following SEC on a Superdex 200 16/600 column. (B) Thermal stability of eight ExpiCHO-expressed UFO-BG trimers derived from five subtypes by differential scanning calorimetry (DSC). (C) Thermal stability of four ExpiCHO-expressed UFO trimers derived from four subtypes by DSC. (D) Thermal stability of 293 F-expressed BG505 UFO trimer and DU172.17 UFO-BG trimer by DSC. In (B)-(D), three thermal parameters (T_m , $T_{1/2}$ and T_{onset}) are labeled on the DSC profiles. Data fitting was performed using the standard software provided by the vendor. The raw data and the fitted curve are plotted as black dotted lines and red lines, respectively. (E) A CN54 gp140 construct with 14 mutations (termed CN54M14). CN54M14 sequence with the 14 mutations shown in red and lower case, the N332 and SOS mutations in blue, the generic HR1 design ((GS)₄) in cyan, and the cleavage site linker ((G₄S)₂) in green. SEC profiles of wild-type CN54 SOSIP, CN54M14 UFO, and CN54M14 UFO-BG trimers following transient expression in 1L 293 F cells, GNL purification, and SEC on a Superdex 200 10/300 column. (F) SEC profiles of UFO-BG trimers derived from clades B, C, and B/C following transient expression in 1L 293 F cells, GNL purification, and SEC on a Superdex 200 10/300 column.

A



B

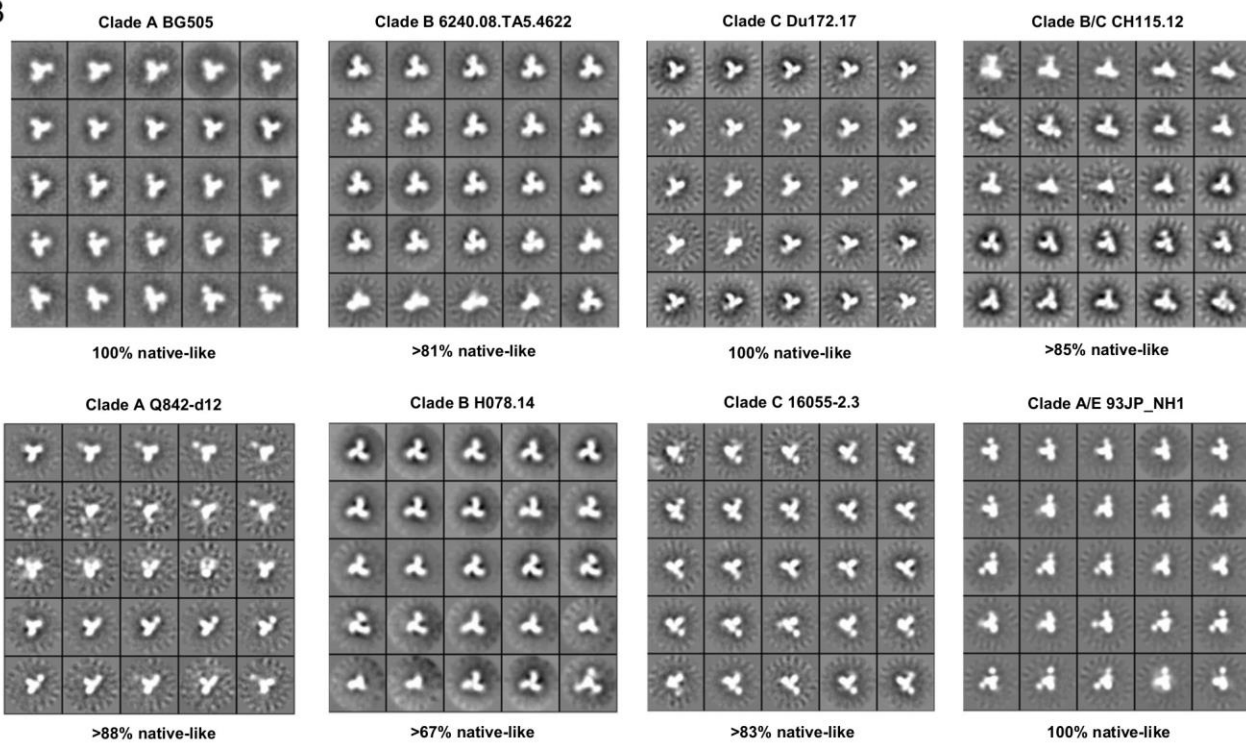
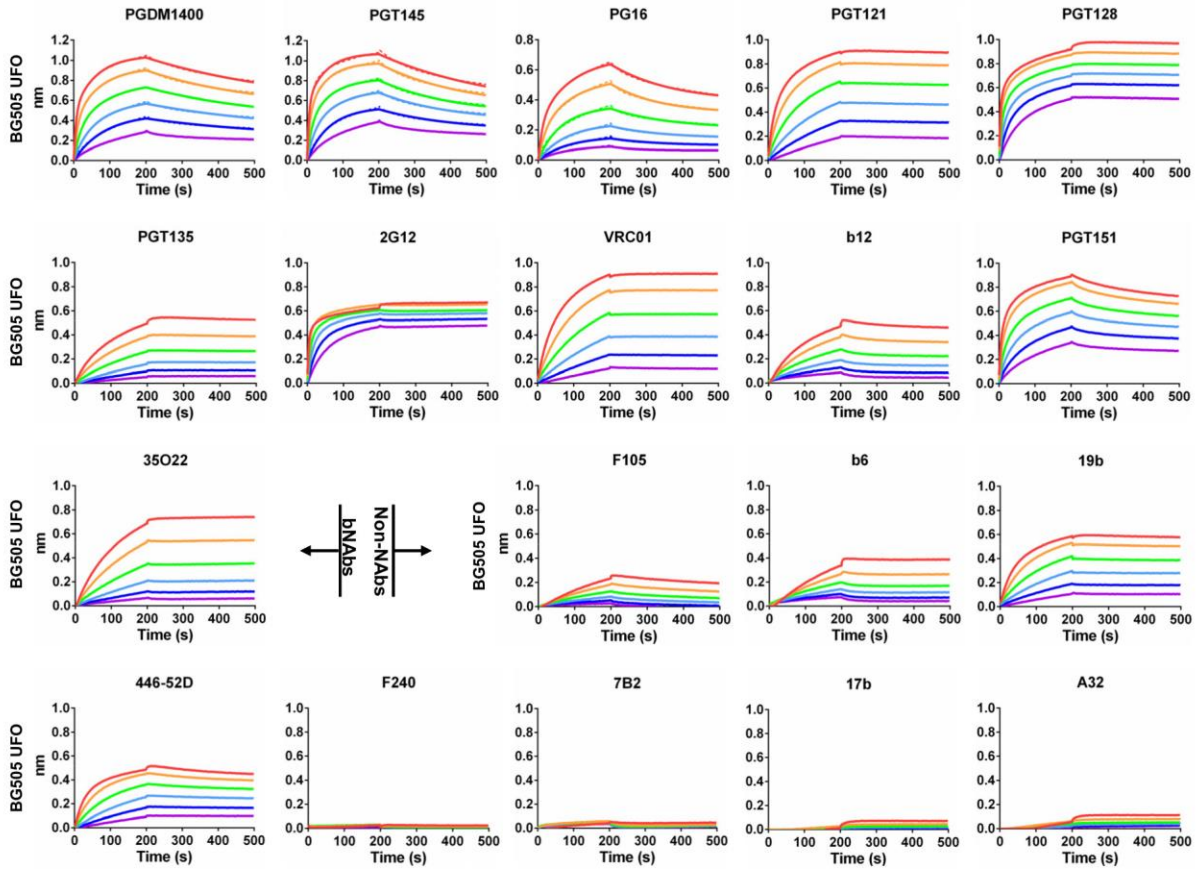
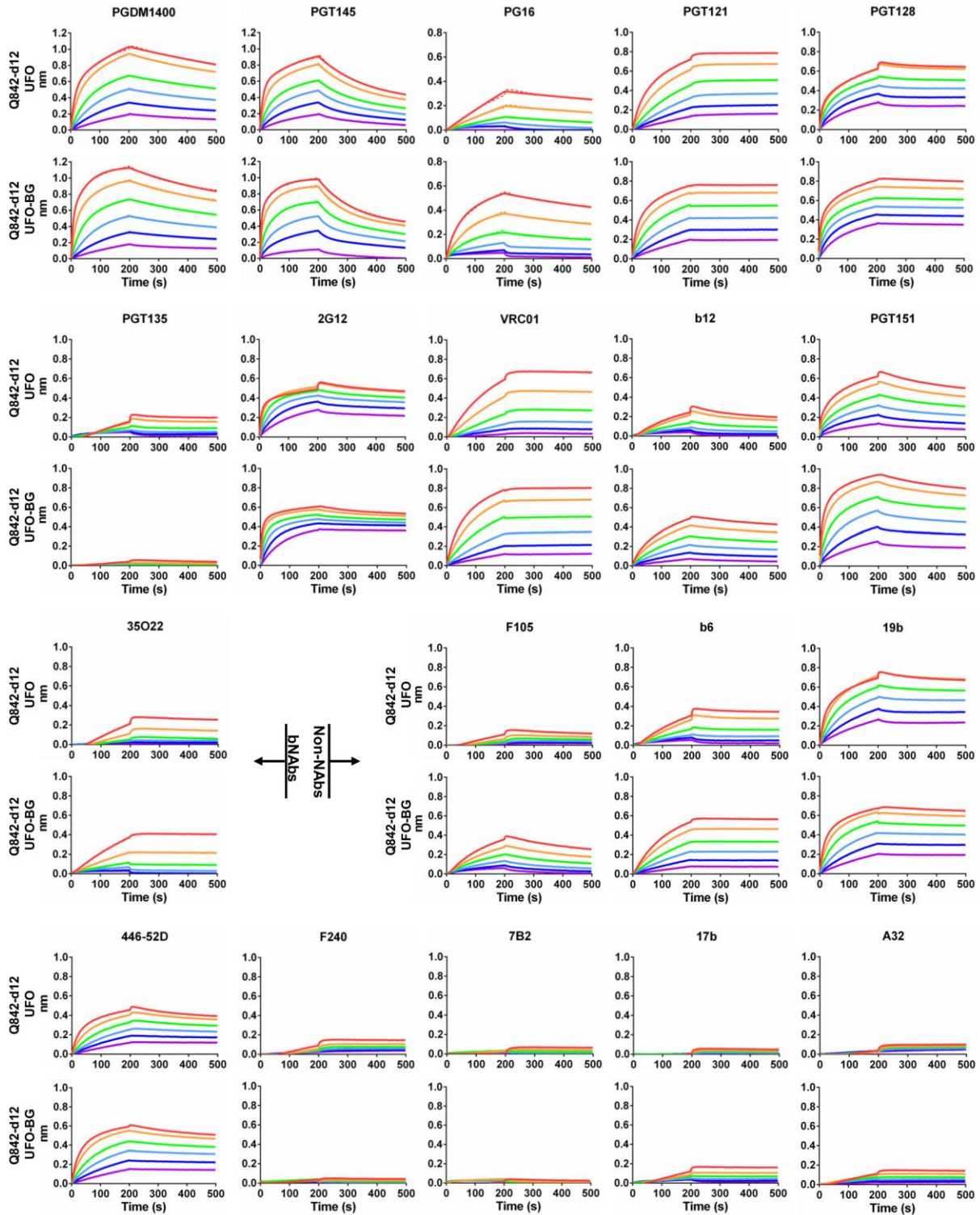


Fig. S3. Structural characterization of diverse UFO-BG trimers. (A) Crystal structure of clade B tier 3 H078.14 UFO-BG trimer bound to bNAbs PGT124 and 35O22 at 4.6 Å resolution. A 2Fo-Fc electron density map (contoured at 1.0 σ) showing gp120 (in yellow backbone tube model) and gp41_{ECTO} (in green backbone tube model) of the H078.14 UFO-BG protomer in the crystal asymmetric unit bound to PGT124 (grey and pink) and 35O22 (cyan and magenta). (B) Negative-stain EM of UFO-BG trimers produced in ExpiCHO cells followed by GNL and SEC purification. The full sets of reference-free 2D class averages are shown for clade A BG505 (tier 2) and Q842-d12 (tier 2), clade B 6240.08.TA5.4622 (tier 2) and H078.14 (tier 2), clade C Du172.17 (tier 2) and 16055-2.3 (tier 2), clade B/C CH115.12 (tier 3) and clade A/E 93JP_NH1. The percentage of native-like trimers is indicated below each panel.

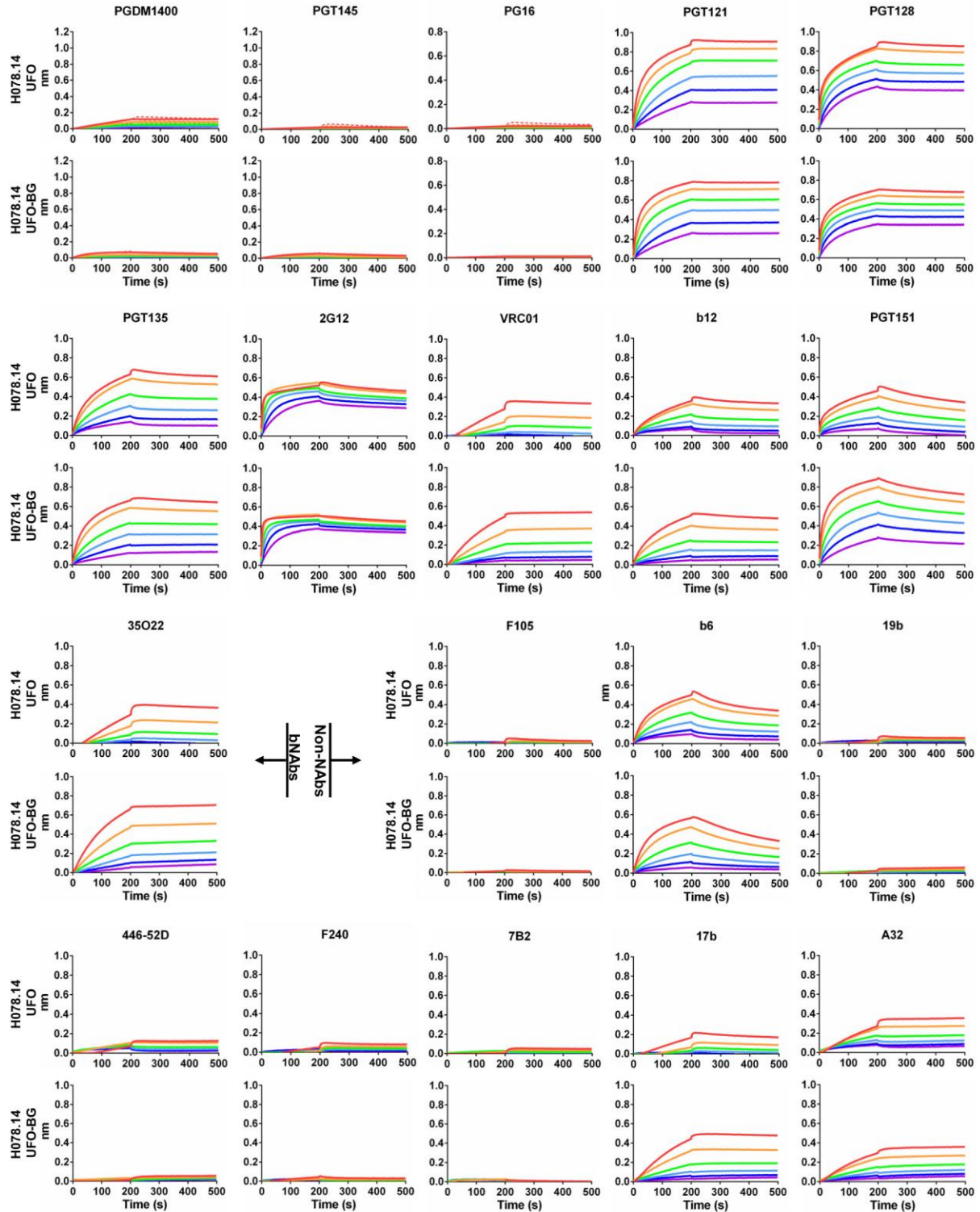
A



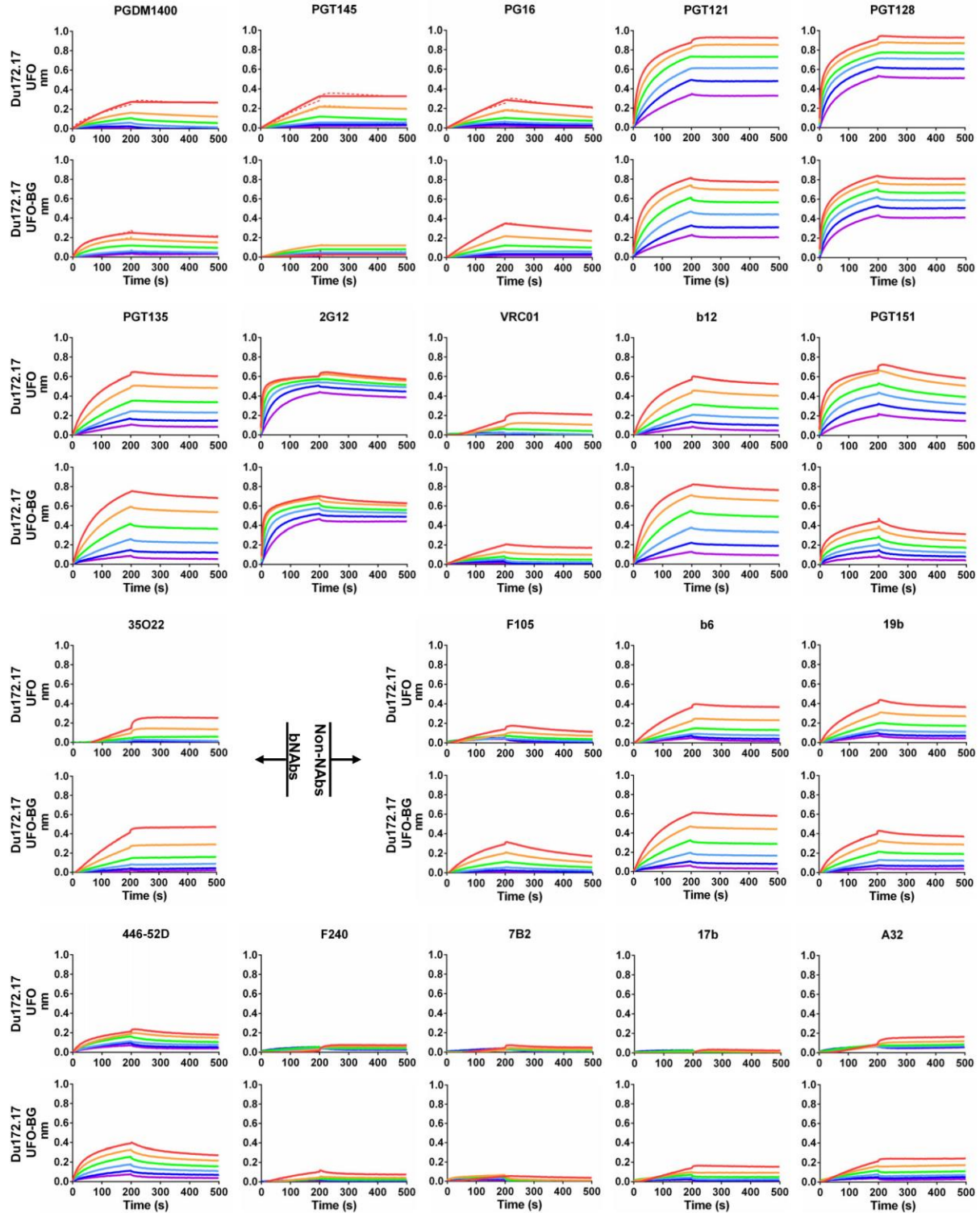
B



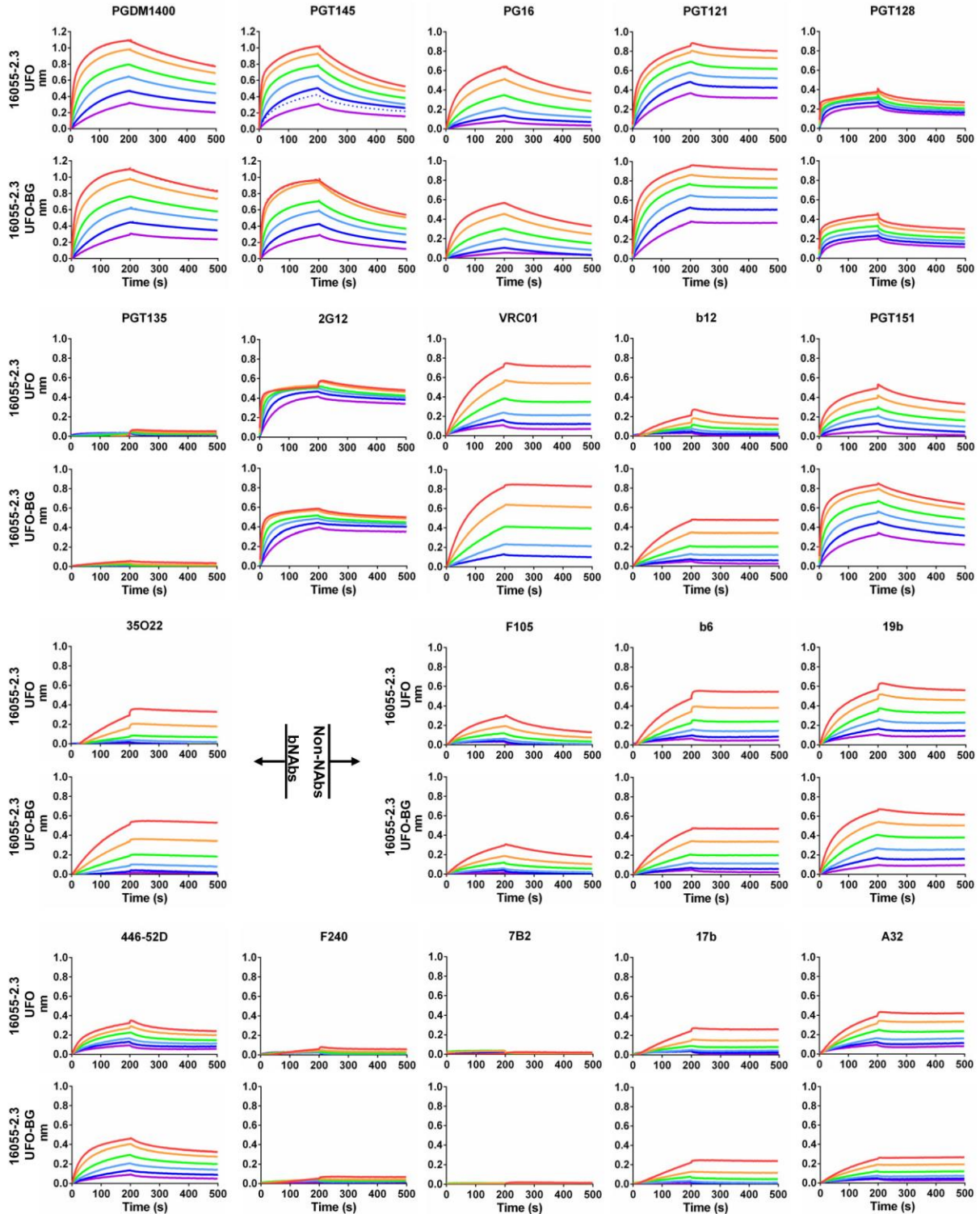
D



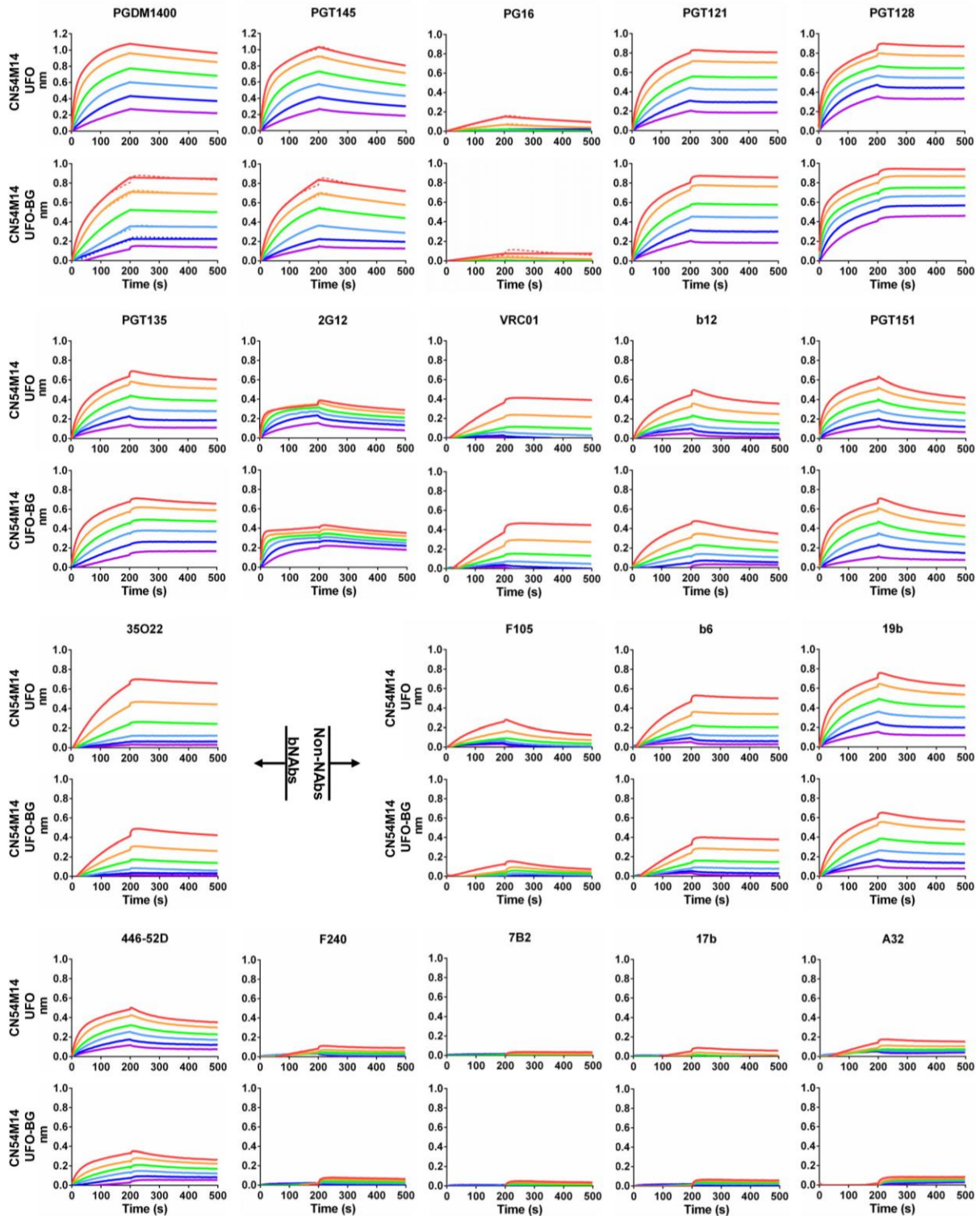
E



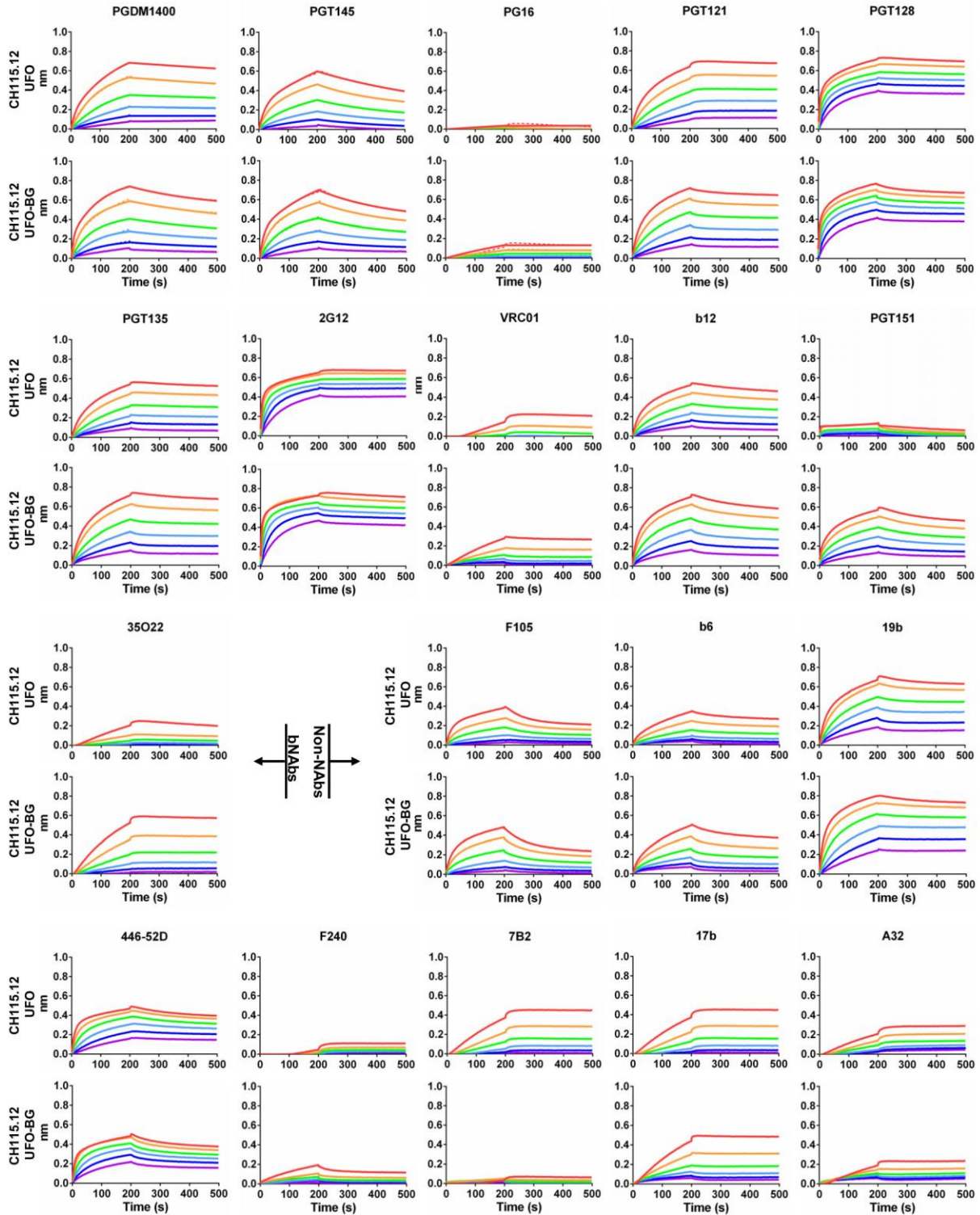
F



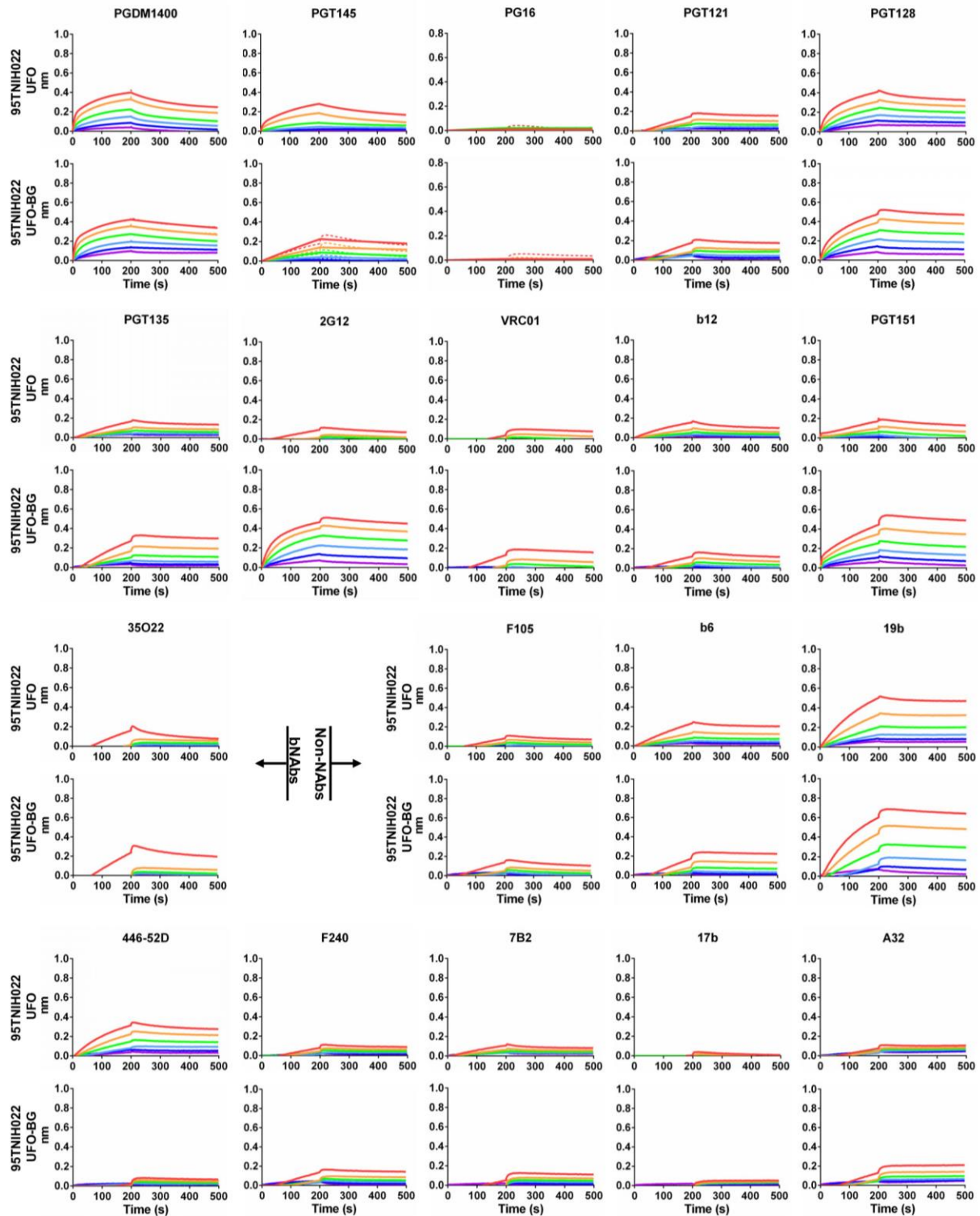
G



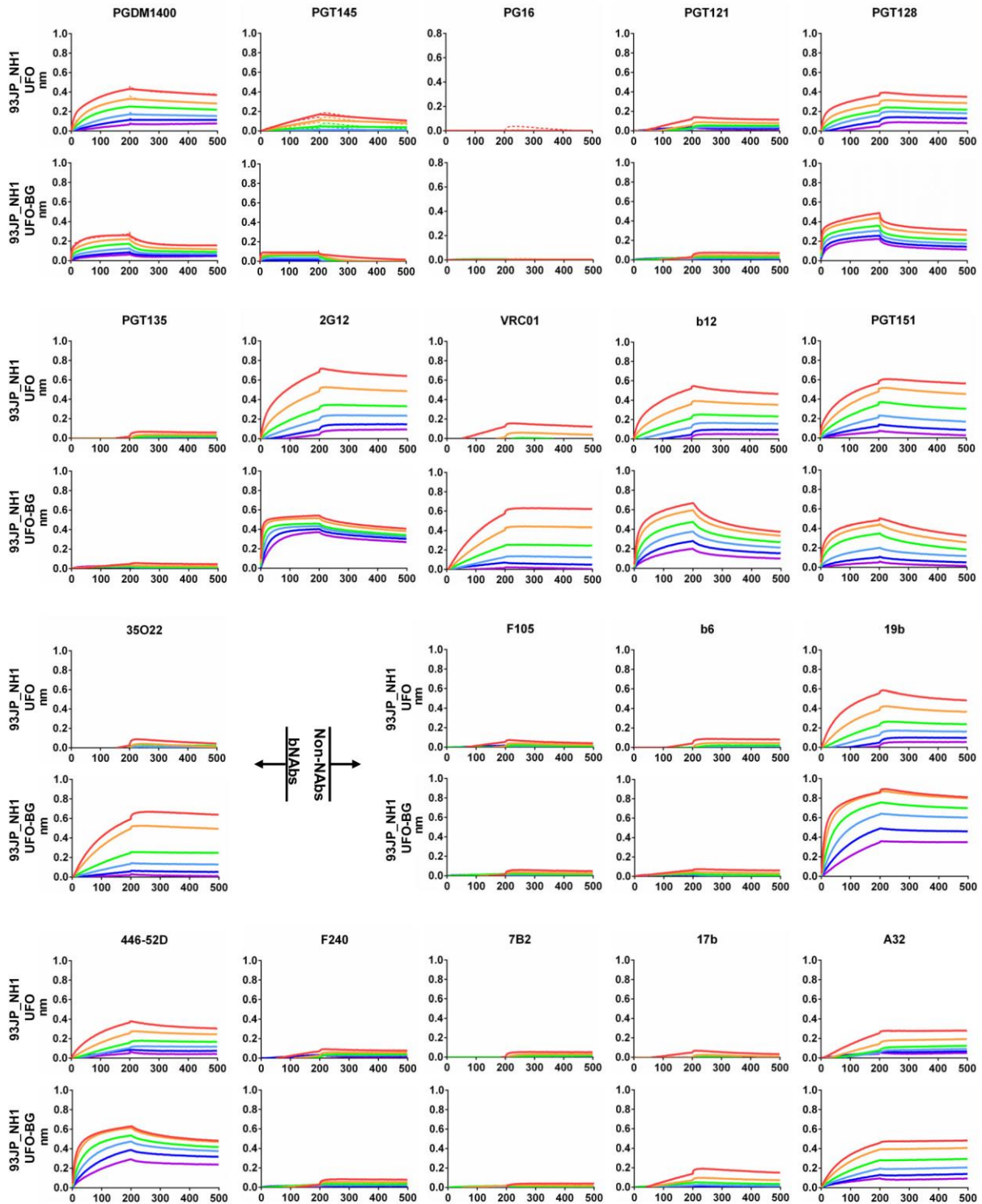
H



1



J



K

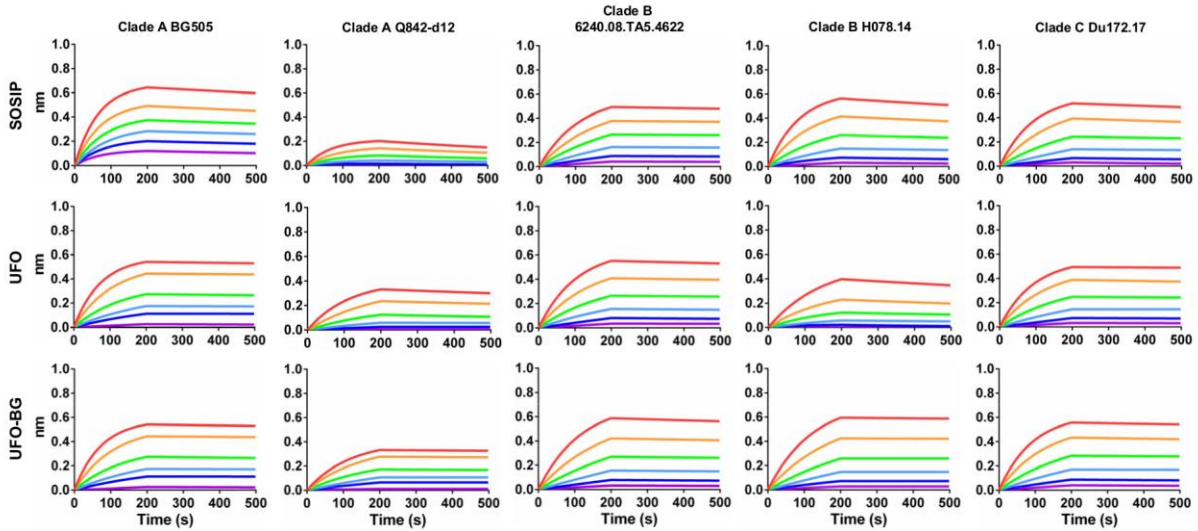
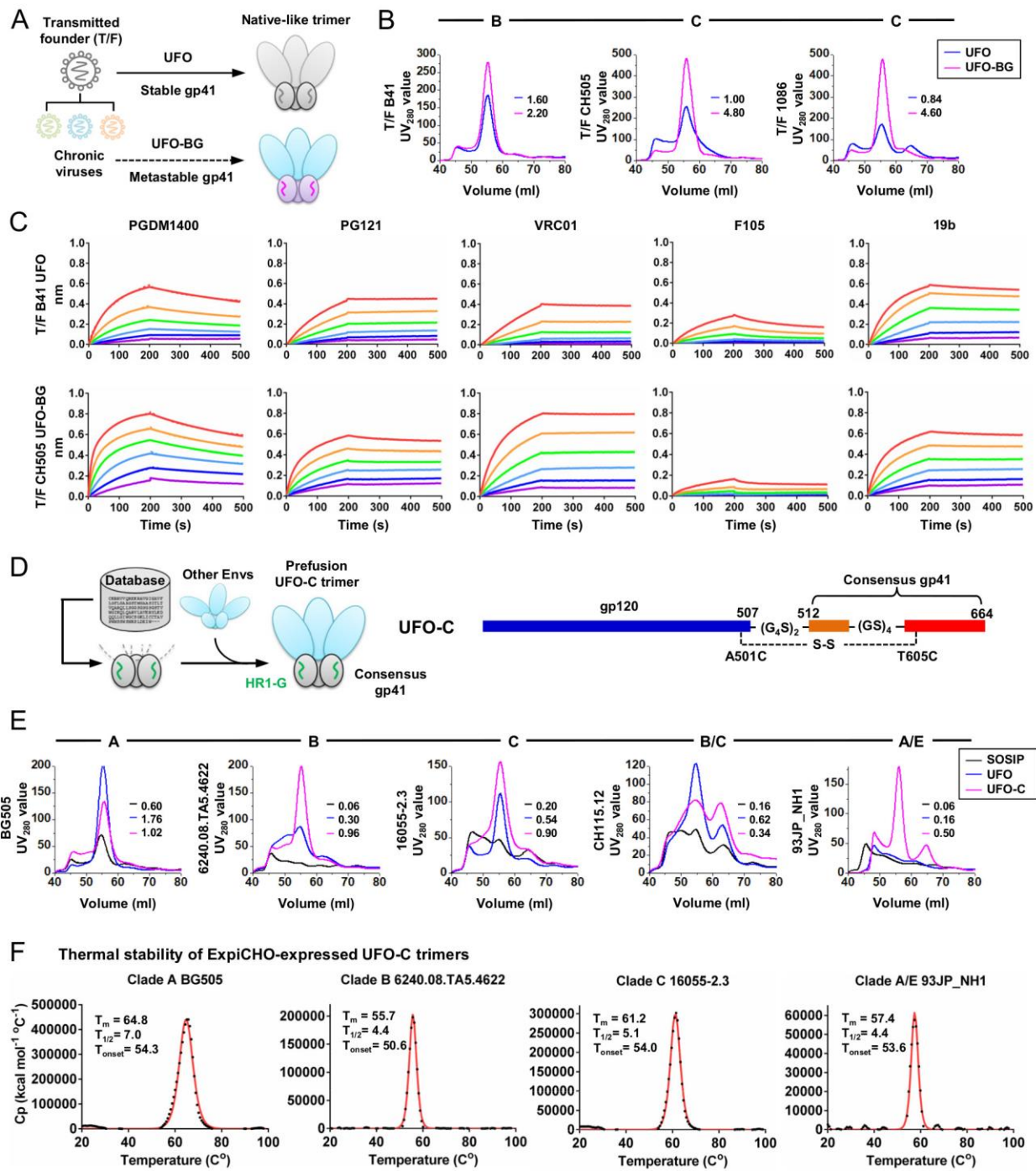
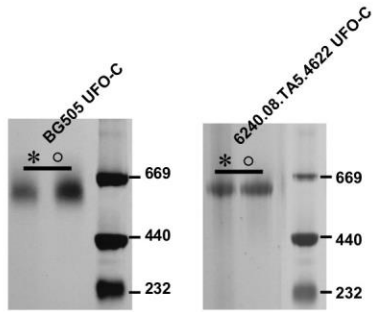


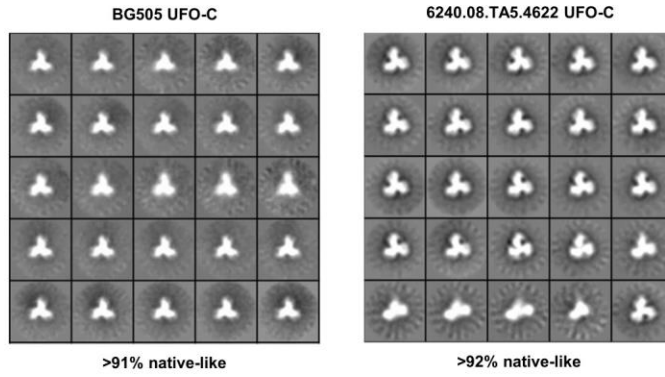
Fig. S4. Antigenic profiles of UFO and UFO-BG trimers derived from 10 strains of five subtypes assessed against a panel of 11 bNAbs, 8 non-NAbs, and CD4-Ig. Sensorgrams were obtained from an Octet RED96 instrument using a titration series of six trimer concentrations (200-6.25 nM by 2-fold dilution). The strains tested for antibody binding include (A) clade A BG505 (tier 2), (B) clade A Q842-d12 (tier 2), (C) clade B 6240.08.TA5.4622 (tier 2), (D) clade B H078.14 (tier 2), (E) clade C Du172.17 (tier 2), (F) clade C 16055-2.3 (tier 2), (G) clade B/C CN54 with 14 mutations (CN54M14, see fig. S2E), (H) clade B/C CH115.12 (tier 3), (I) clade A/E 95TNIH022, and (J) clade A/E 93JP_NH1. (K) CD4-Ig binding to SOSIP, UFO, and UFO-BG trimers measured for five selected Envs of clades A, B, and C. BLI was performed using the same protocol as described above for antibodies.



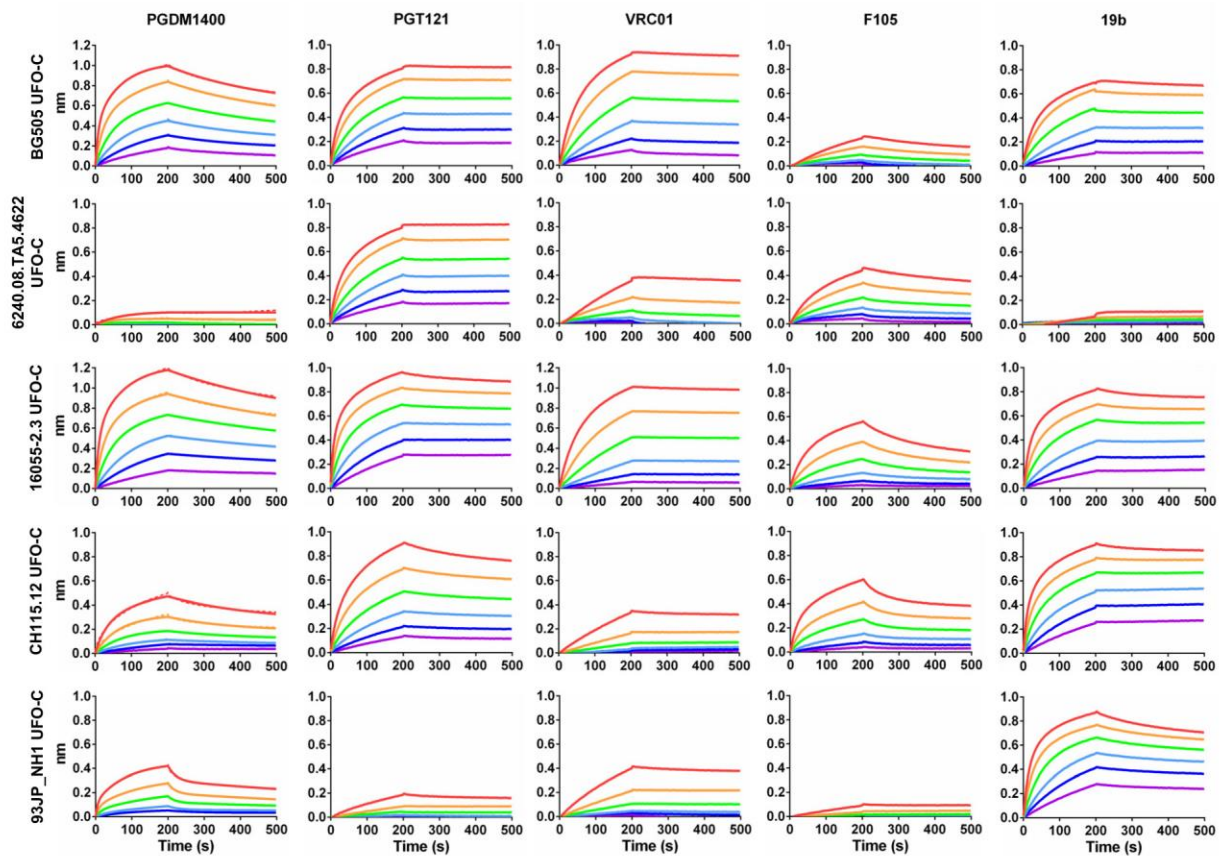
G



H

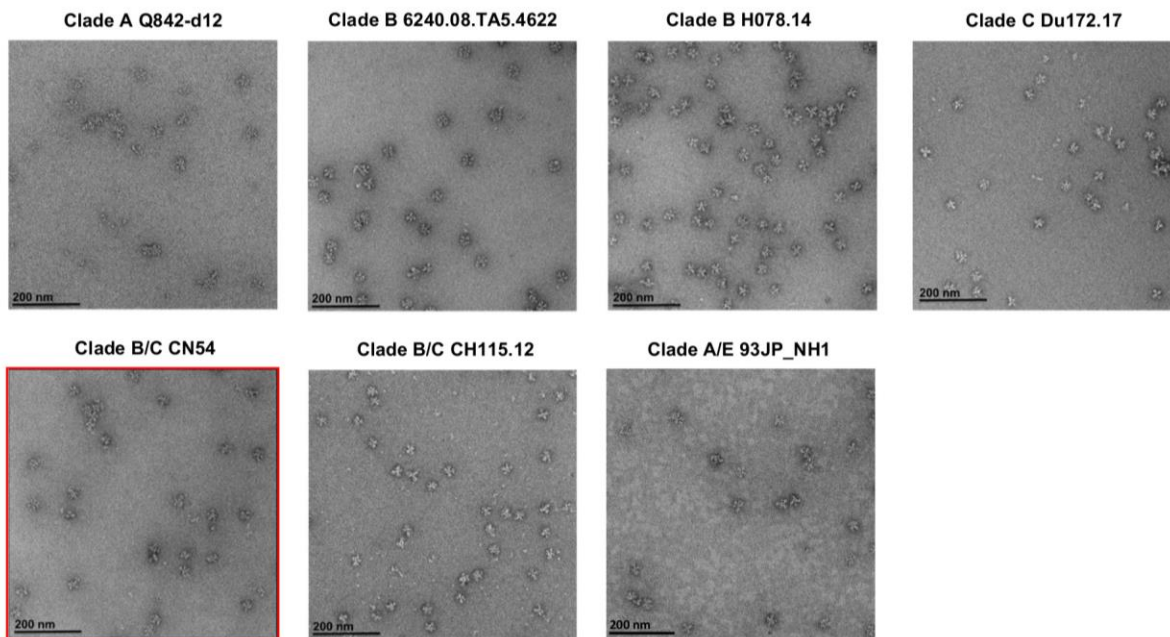
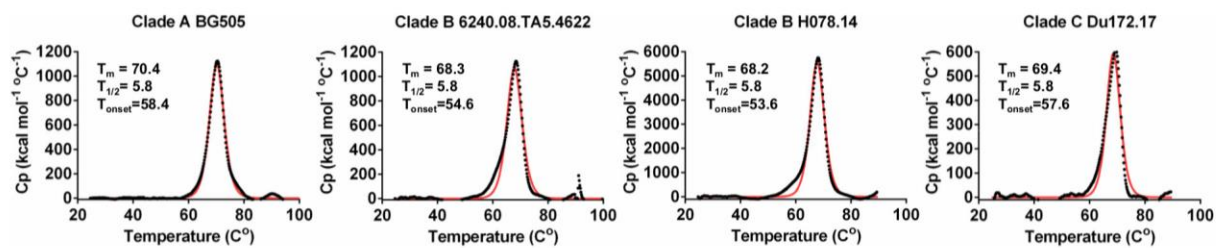


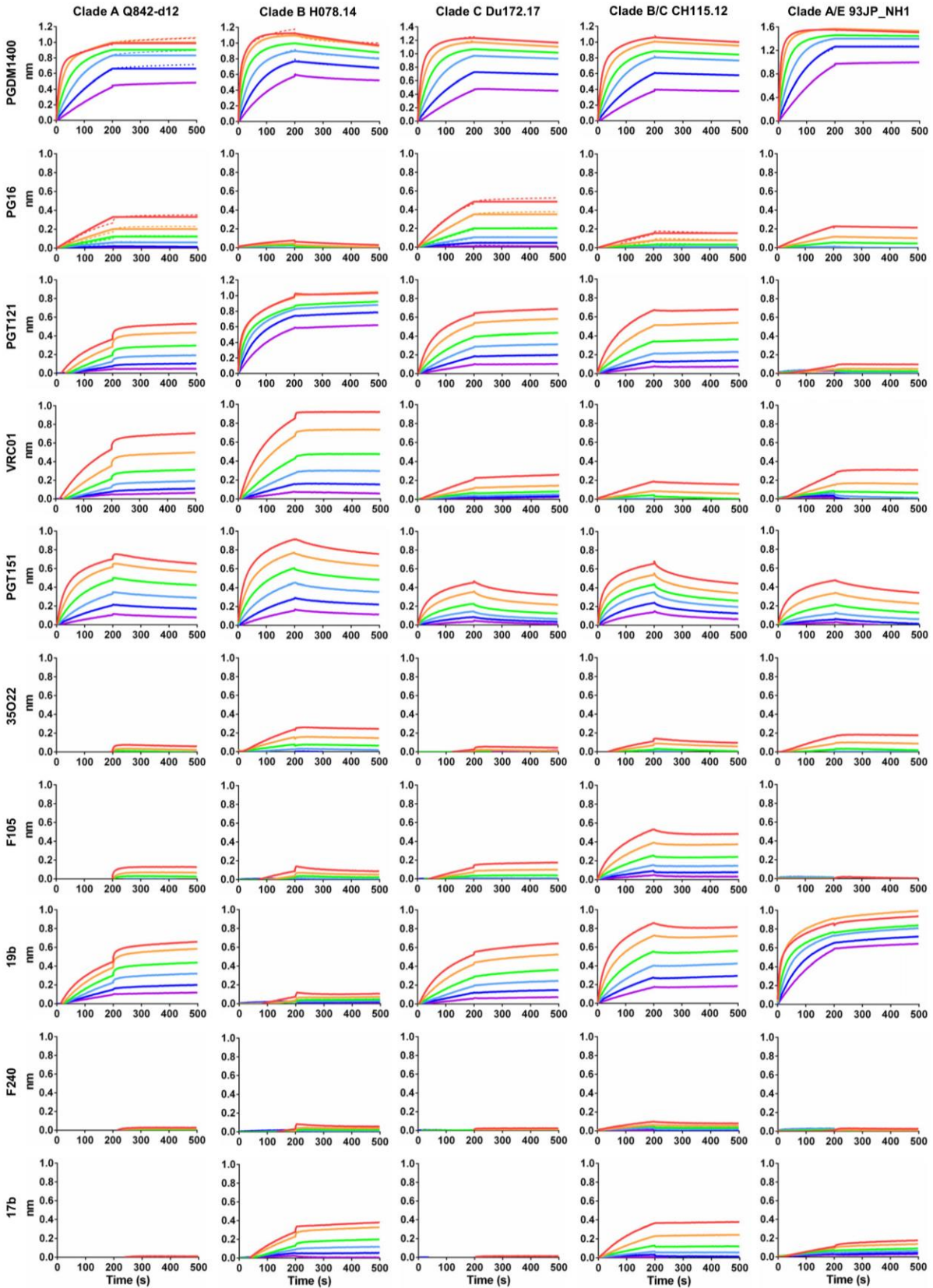
I



	BG505	6240.08.TA5.4622	16055-2.3	CH115.12	93JP_NH1
PGDM1400	1.0	0.1	1.2	0.5	0.4
PGT121	0.8	0.8	1.0	0.9	0.4
VRC01	0.9	0.4	1.0	0.4	0.2
F105	0.2	0.5	0.6	0.6	0.1
19b	0.7	0.1	0.8	0.9	0.9

Fig. S5. Evolutionary root of metastability and design of UFO-C trimers containing a database-derived ancestral gp41_{ECTO}. (A) Connection between HIV-1 evolution and Env metastability. (B) SEC profiles of UFO and UFO-BG trimers derived from three transmitted/founder (T/F) viruses, including clade B B41, clade C CH505, and clade C 1086. The yield (mg) of SEC-purified trimer protein (fractions corresponding to 53-57ml) obtained from 100-ml ExpiCHO expression is listed for both trimer designs. (C) Antigenic profiles of B41 UFO and CH505 UFO-BG trimers measured against three bNAbs and two non-NAbs. Sensorgrams were obtained on an Octet RED96 using a trimer titration series of six concentrations (200-6.25 nM by two-fold dilution). (D) Design (left) and schematic representation (right) of the UFO-C trimers. As shown on the left, a database-derived consensus gp41_{ECTO} in conjunction of a generic UFO design is used to stabilize gp120s from diverse HIV-1 Envs in a hybrid form of gp140 trimer designated UFO-C. The generic HR1 redesign, an 8-aa (GS)₄ linker, is highlighted in green. (E) SEC profiles of UFO-C trimers derived from five representative stains of clade A, B, C, B/C, and A/E origins. The yield (mg) of SEC-purified trimer protein (fractions corresponding to 53-57ml) obtained from 100-ml ExpiCHO expression is listed for each of the three trimer designs (SOSIP, UFO, and UFO-C). (F) Thermal stability of 4 ExpiCHO-expressed UFO-C trimers derived from four subtypes by differential scanning calorimetry (DSC). Three thermal parameters (T_m , $T_{1/2}$ and T_{onset}) are labeled on the DSC profiles. Data fitting was performed using the standard software provided by the vendor. The raw data and the fitted curve are plotted as black dotted lines and red lines, respectively. (G) BN-PAGE of Env protein after GNL purification but prior to SEC and of purified trimer following SEC and BN-PAGE for two UFO-C constructs derived from clade A BG505 and clade B 6240.08.TA5.4622. (H) Reference-free 2D class averages derived from negative-stain EM of the BG505 and 6240.08.TA5.4622 UFO-C trimers. Percentage of native-like trimers is indicated below each panel. (I) Antigenic profiles of five purified UFO-C trimers measured against three bNAbs and two non-NAbs. Sensorgrams were obtained on an Octet RED96 using a trimer titration series of six concentrations (200-6.25 nM by two-fold dilution). The strains tested here include clade A BG505 (tier 2), clade B 6240.08.TA5.4622 (tier 2), clade C 16055-2.3 (tier 2), clade B/C CH115.12 (tier 3), and clade A/E 93JP_NH1. The peak values at the highest concentration are summarized in a matrix, in which cells are colored in red and green for bNAbs and non-NAbs, respectively. Higher color intensity indicates greater binding signal measured by Octet.

A**B**

C

D

Sequence alignment

```

1VLW MKMEELFKKHKIVAVLRANSVEEAKKALAVFEGGVHLIEITFTVPDADTVIKELSFLEKGAIIAGAGTTSVEQCRKAVESGAEFIVSPHLDEEISQFCKEKGVFYPGVMPTPELVKA
5KP9 MKMEELFKKHKIVAVLRANSVEEAKKALAVFEGGVHLIEITFTVPDADTVIKELSFLEKGAIIAGAGTTSVEQCRKAVESGAEFIVSPHLDEEISQFCKEKGVFYPGVMPTPELVKA
*****:*****

1VLW MKLGHTILKLFPGEEVVGQPFVKAMKGFPPNVKFPVPTGGVNLNDVCEWFKAGVLA VGVGSALVKGTPDEVREKAKAFVEKIRGCTE
5KP9 MKLGHTILKLFPGEEVVGQPFVKAMKGFPPNVKFPVPTGGVNLNDVCEWFKAGVLA VGVGSALVKGTPDEVREKAKAFVEKIRGCTE
*****:*****
  
```

E

```

>1VLW-V1
MKMEELFKKHKIVAVLRANSVEEAKKALHVFSGGVHLIEITFTVPDADTVIKELSFLEKGAIIAGAGTTSVEQCRKAVESGAEFIVSPHLDEEISQFCKEKGVFYPGVMPTPELVKA
MKLGHTILKLFPGEEVVGQPFVKAMKGFPPNVKFPVPTGGVNLNDVCEWFKAGVLA VGVGSALVKGTWDEVSRKAKAFVEKIRGCTE

>1VLW-V2
MKMEELFKKHKIVAVLRANSVEEAKKALHVFEGGVHLIEITFTVPDADTVIKELSFLEKGAIIAGAGTTSVEQCRKAVESGAEFIVSPHLDEEISQFCKEKGVFYPGVMPTPELVKA
MKLGHTILKLFPGEEVVGQPFVKAMKGFPPNVKFPVPTGGVNLNDVCEWFKAGVLA VGVGSALVKGTWHEVAAKAKAFVEKIRGCTE

>1VLW-V3
MKMEELFKKHKIVAVLRANSVEEAKKALHVFEGGVHLIEITFTVPDADTVIKELSFLEKGAIIAGAGTTSVEQCRKAVESGAEFIVSPHLDEEISQFCKEKGVFYPGVMPTPELVKA
MKLGHTILKLFPGEEVVGQPFVKAMKGFPPNVKFPVPTGGVNLNDVCEWFKAGVLA VGVGSALVKGTWDEVAAKAKAFVEKIRGCTE

>1VLW-V4
MKMEELFKKHKIVAVLRANSVEEAKKALAVFLAGVHLIEITFTVPDADTVIKELSFLEKGAIIAGAGTTSVEQCRKAVESGAEFIVSPHLDEEISQFCKEKGVFYPGVMPTPELVKA
MKLGHTILKLFPGEEVVGQPFVKAMKGFPPNVKFPVPTGGVNLNDVCEWFKAGVLA VGVGSALVKGTVEVAAKAAAFVEKIRGCTE

>1VLW-V5
MKMEELFKKHKIVAVLRANSVEEAKKALAVFLGGVHLIEITFTVPDADTVIKELSFLEKGAIIAGAGTTSVEQCRKAVESGAEFIVSPHLDEEISQFCKEKGVFYPGVMPTPELVKA
MKLGHTILKLFPGEEVVGQPFVKAMKGFPPNVKFPVPTGGVNLNDVCEWFKAGVLA VGVGSALVKGTVEVAAKAAAFVEKIRGCTE

>1VLW-V6
MKMEELFKKHKIVAVLRANSVEEAKKALAVFLGGVHLIEITFTVPDADTVIKELSFLEKGAIIAGAGTTSVEQCRKAVESGAEFIVSPHLDEEISQFCKEKGVFYPGVMPTPELVKA
MKLGHTILKLFPGEEVVGQPFVKAMKGFPPNVKFPVPTGGVNLNDVCEWFKAGVLA VGVGSALVKGTVEVAAKAAAFVEKIRGCTE

>1VLW-V7
MKMEELFKKHKIVAVLRANSVEEAKKALAVFLGGVHLIEITFTVPDADTVIKELSFLEKGAIIAGAGTTSVEQCRKAVESGAEFIVSPHLDEEISQFCKEKGVFYPGVMPTPELVKA
MKLGHTILKLFPGEEVVGQPFVKAMKGFPPNVKFPVPTGGVNLNDVCEWFKAGVLA VGVGSALVKGTVEVAAKAAAFVEKIRGCTE

>1VLW-V8
MKMEELFKKHKIVAVLRANSVEEAKKALHVFEGGVHLIEITFTVPDADTVIKELSFLEKGAIIAGAGTTSVEQCRKAVESGAEFIVSPHLDEEISQFCKEKGVFYPGVMPTPELVKA
MKLGHTILKLFPGEEVVGQPFVKAMKGFPPNVKFPVPTGGVNLNDVCEWFKAGVLA VGVGSALVKGTWAEVAAKAKAFVEKIRGCTE

>1VLW-V9
MKMEELFKKHKIVAVLRANSVEEAKKALAVFVGGVHLIEITFTVPDADTVIKELSFLEKGAIIAGAGTTSVEQCRKAVESGAEFIVSPHLDEEISQFCKEKGVFYPGVMPTPELVKA
MKLGHTILKLFPGEEVVGQPFVKAMKGFPPNVKFPVPTGGVNLNDVCEWFKAGVLA VGVGSALVKGTIAEVAAKAAAFVEKIRGCTE

>1VLW-V10
MKMEELFKKHKIVAVLRANSVEEAKKALAVFVGGVHLIEITFTVPDADTVIKELSFLEKGAIIAGAGTTSVEQCRKAVESGAEFIVSPHLDEEISQFCKEKGVFYPGVMPTPELVKA
MKLGHTILKLFPGEEVVGQPFVKAMKGFPPNVKFPVPTGGVNLNDVCEWFKAGVLA VGVGSALVKGTVEVAAKAAAFVEKIRGCTE
  
```

F

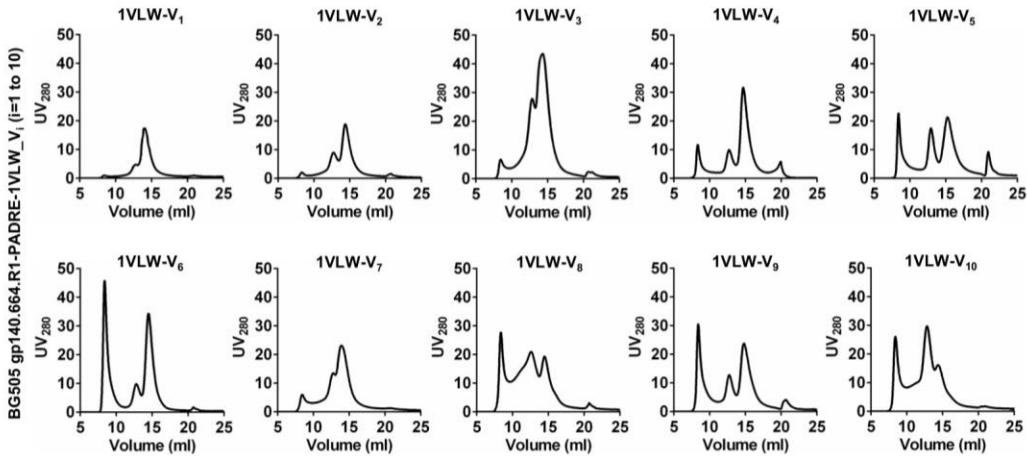
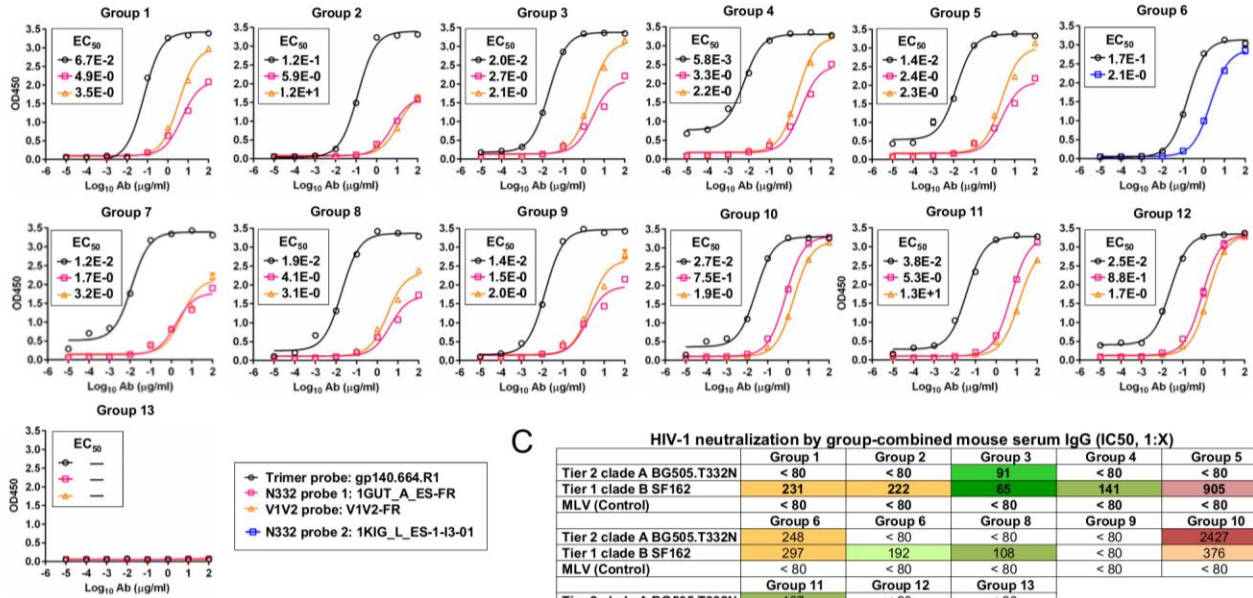
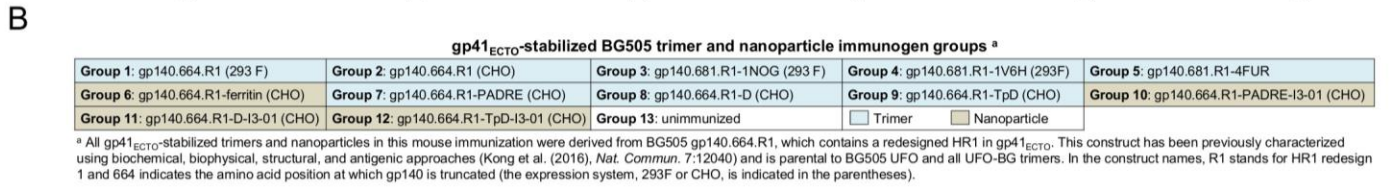
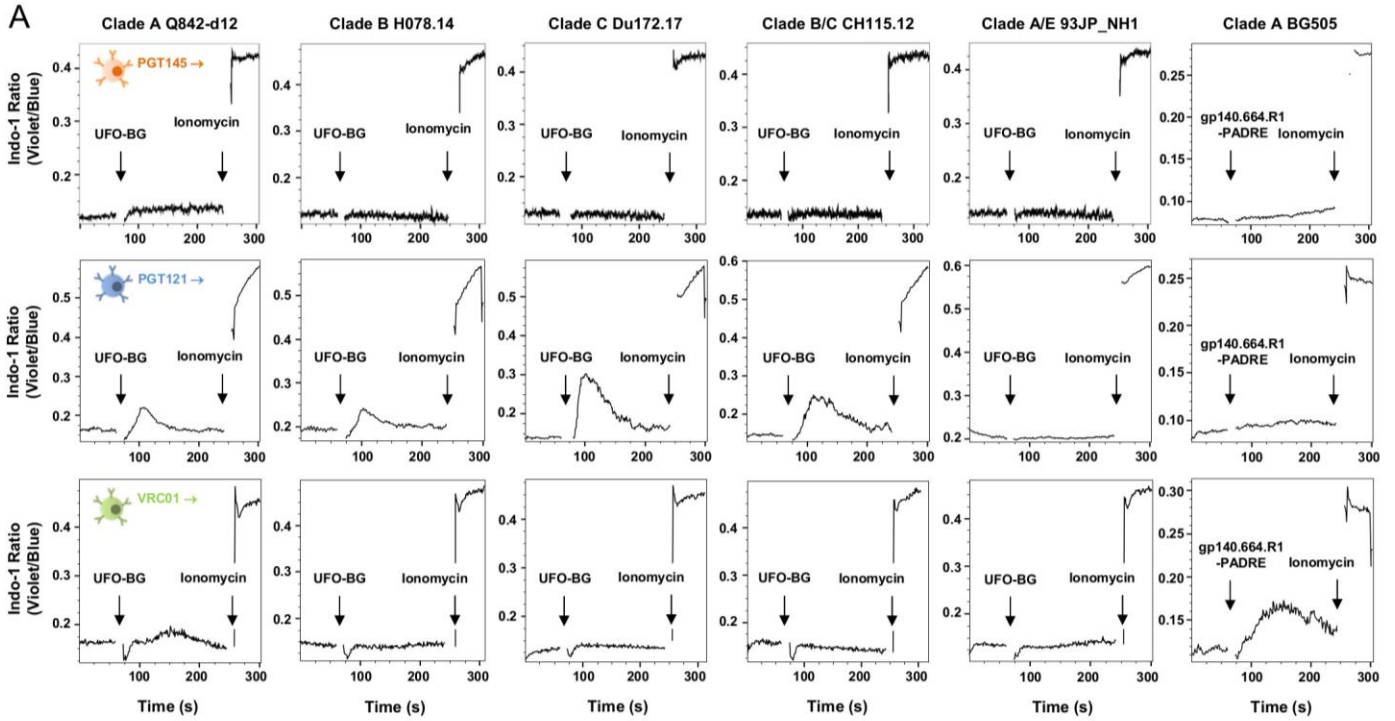


Fig. S6. Characterization of gp41_{ECTO}-stabilized trimer-presenting nanoparticles.

(A) Micrographs derived from negative-stain EM of UFO-BG-FR nanoparticles of five subtypes. (B) Thermal stability of four UFO-BG-FR nanoparticles derived from three subtypes by differential scanning calorimetry (DSC). Three thermal parameters (T_m , $T_{1/2}$ and T_{onset}) are labeled on the DSC profiles. Data fitting was performed using the standard software provided by the vendor. The raw data and the fitted curve are plotted as black dotted lines and red lines, respectively. (C) Antigenic profiles of UFO-BG-FR nanoparticles derived from five subtypes evaluated against a panel of six bNAbs and four non-NAbs. Sensorgrams were obtained from an Octet RED96 instrument using a titration series of 6 concentrations (starting at 35 nM by 2-fold dilution). The strains tested here include clade A Q842-d12 (tier 2), clade B H078.14 (tier 2), clade C Du172.17 (tier 2), clade B/C CH115.12 (tier 3), and clade A/E 93JP_NH1. (D) Sequence alignment of I3-01 (PDBID: 5KP9) and 2-dehydro-3-deoxyphosphogluconate aldolase/4-hydroxy-2-oxoglutarate aldolase (TM0066) from *Thermotoga maritima* (PDBID: 1VLW), with the five amino acids that differ in the two sequences colored in red and the 11 amino acids at the I3-01 particle-forming interface highlighted in yellow. (E) Sequences of ten 1VLW variants (1VLW-V_i, i=1 to 10) by altering amino acids at the corresponding I3-01 particle-forming interface. (F) SEC profiles of ten BG505 gp140.664.R1-PADRE-1VLW-V_i constructs obtained from a Superose 6 10/300 GL column. The fusion constructs were expressed in ExpiCHO cells and purified using a 2G12 affinity column.

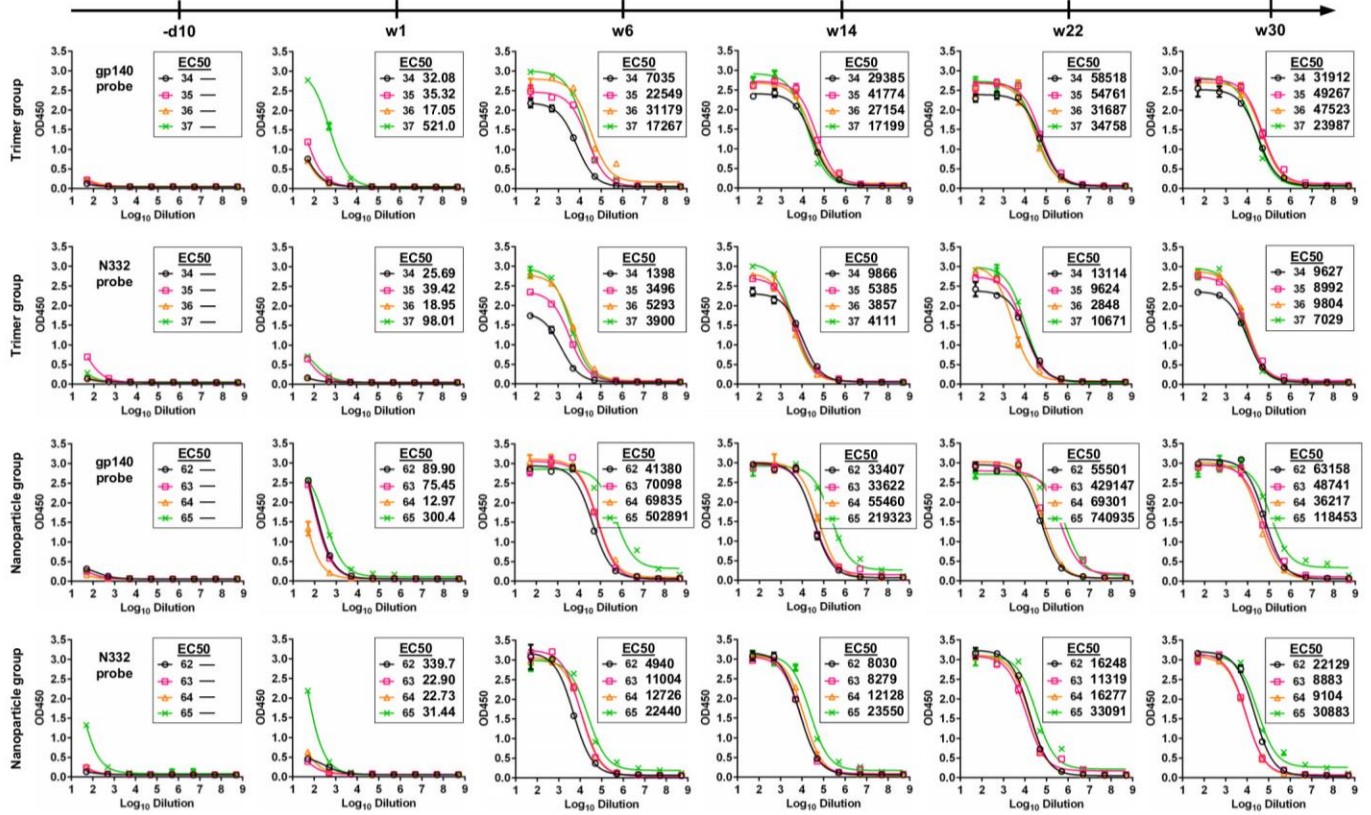


C

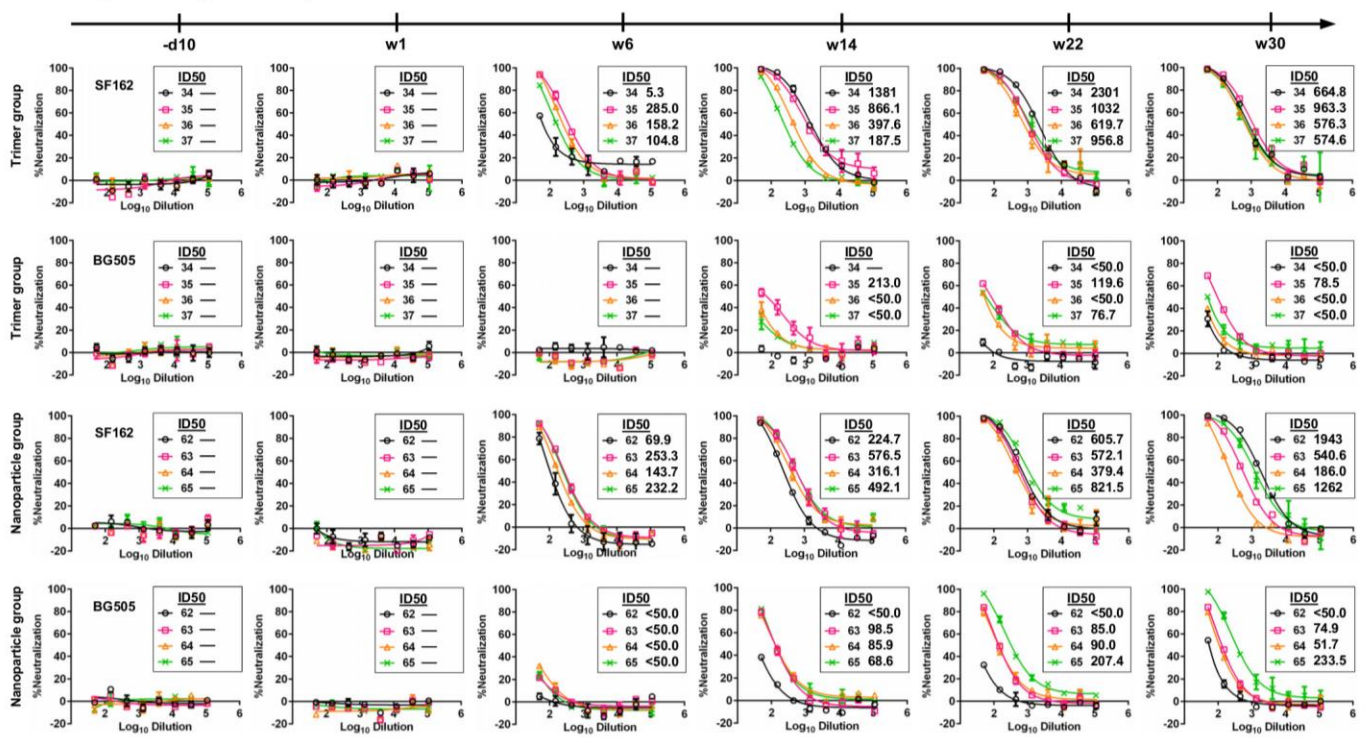
HIV-1 neutralization by group-combined mouse serum IgG (IC₅₀, 1:X)

	Group 1	Group 2	Group 3	Group 4	Group 5
Tier 2 clade A BG505.T332N	< 80	< 80	91	< 80	< 80
Tier 1 clade B SF162	231	222	65	141	905
MLV (Control)	< 80	< 80	< 80	< 80	< 80
	Group 6	Group 6	Group 8	Group 9	Group 10
Tier 2 clade A BG505.T332N	248	< 80	< 80	< 80	2427
Tier 1 clade B SF162	297	192	108	< 80	376
MLV (Control)	< 80	< 80	< 80	< 80	< 80
	Group 11	Group 12	Group 13		
Tier 2 clade A BG505.T332N	137	< 80	< 80		
Tier 1 clade B SF162	396	229	< 80		
MLV (Control)	< 80	< 80	< 80		

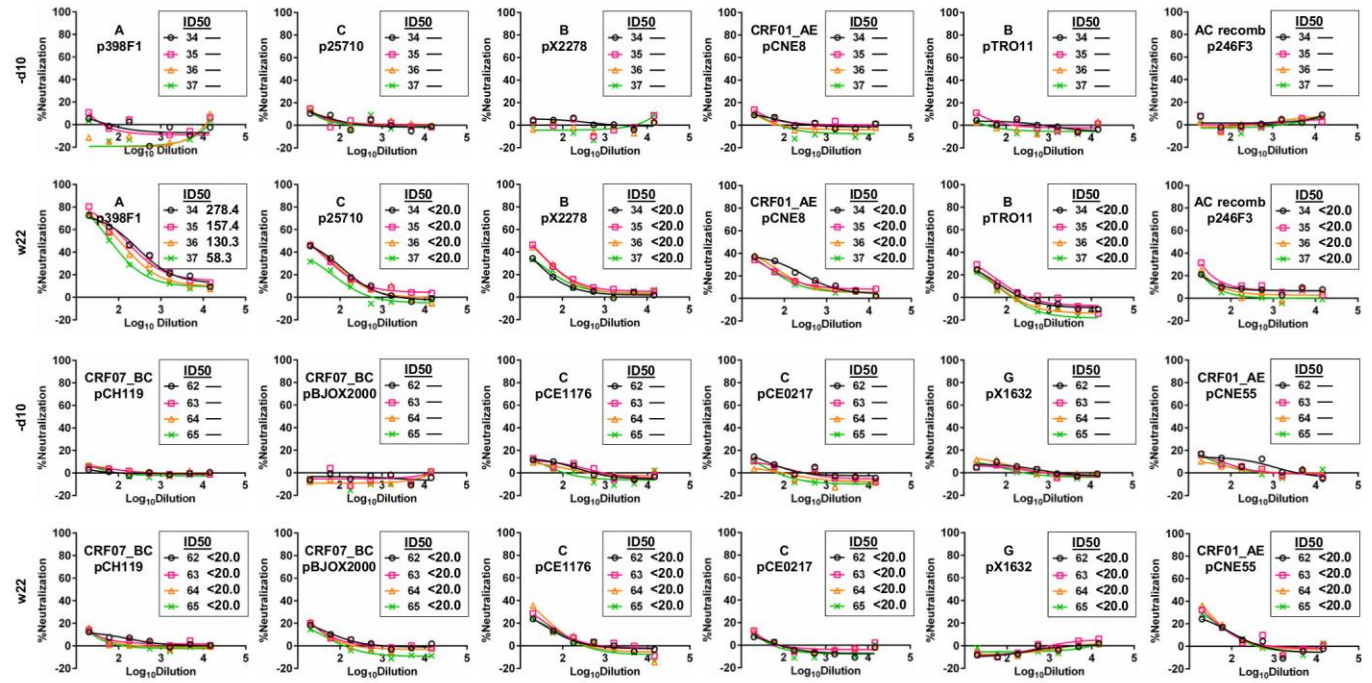
D Longitudinal ELISA analysis of rabbit plasma binding to BG505 UFO trimer and an N332 probe



E Longitudinal analysis of rabbit plasma neutralization of clade A tier 2 BG505.T332N and clade B tier 1 SF162



F Neutralization of global panel by rabbit plasma pre-immunization (-d10) and at week 22 (w22) in the trimer group



G Neutralization of global panel by rabbit plasma pre-immunization (-d10) and at week 22 (w22) in the ferritin group

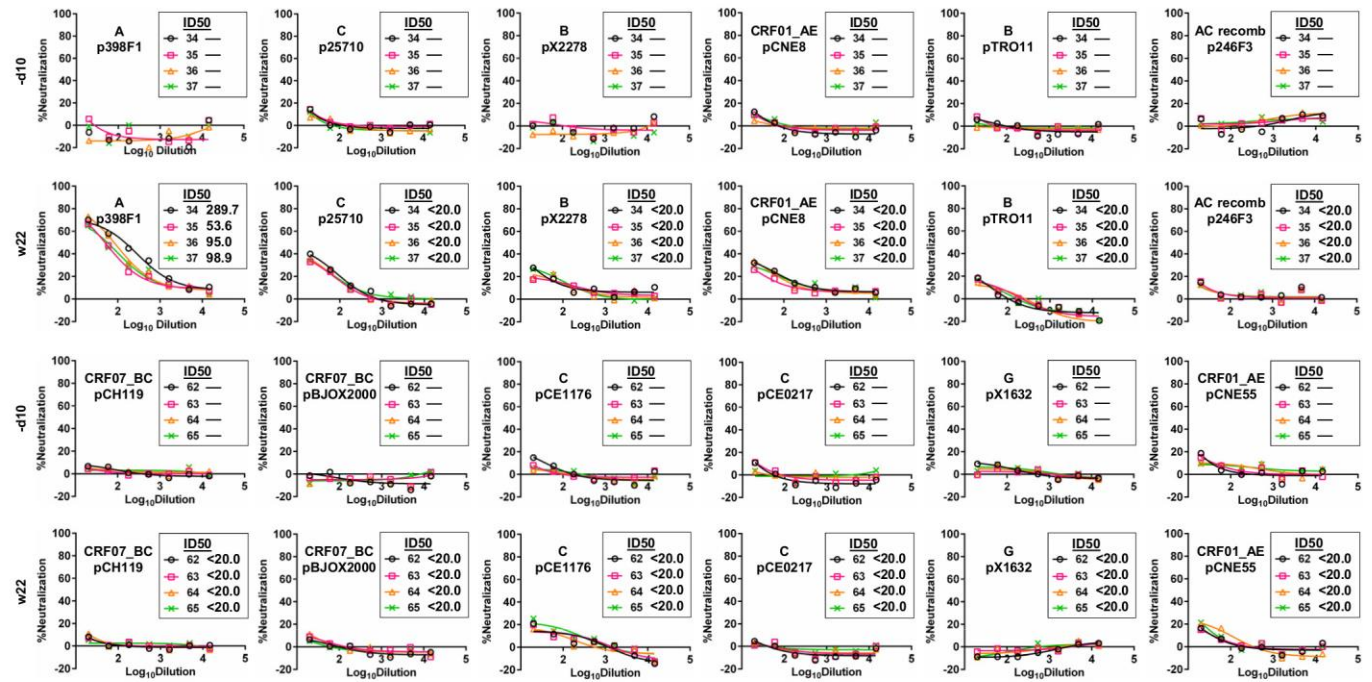


Fig. S7. B cell activation and in vivo evaluation of gp41_{ECTO}-stabilized trimers and nanoparticles. (A) Ca²⁺ mobilization in B cell transfectants carrying PGT145, PGT121, and VRC01 bNAb receptors. WEHI231 cells expressing a doxycyclin-inducible form of bNAb B cell receptor (BCR) were stimulated with anti-BCR antibodies or the indicated antigens at a concentration of 10 µg ml⁻¹: anti-human Ig κ-chain F(ab')₂; anti-mouse IgM; an UFO-BG trimer derived from a clade A, B, C, B/C, or A/E strain, or a gp140-PADRE construct containing a redesigned HR1 bend within gp41_{ECTO}. (B) Testing gp41_{ECTO}-stabilized BG505 trimer and nanoparticle immunogens in mice and ELISA binding of purified mouse IgGs to three HIV-1 antigens, including a BG505 UFO trimer, an N332 supersite probe based on ferritin nanoparticle (1GUT_A_ES-FR) or I3-01 nanoparticle (1KIG_L_ES-2-I3-01), and a V1V2 apex probe based on ferritin nanoparticle (clade C V1V2-FR). EC₅₀ values are labeled for all ELISA plots except for instances in which the highest OD₄₅₀ value is below 0.1 or in cases of ambiguous data fitting. (C) HIV-1 neutralization by group-combined mouse IgGs, with IC₅₀s color-coded according to the value ranging from green (weak neutralization) to red (potent neutralization). (D) ELISA binding of rabbit plasma to BG505 UFO trimer and an I3-01 nanoparticle presenting 60 N332 scaffolds (1KIG_L_ES-2-I3-01). The heat-inactivated plasma was diluted by 50-fold and subjected to a 10-fold dilution series in the assay. EC₅₀ binding antibody titers are labeled for all plots except for the time point of day -10 (-d10). (E) Neutralization of clade A tier 2 BG505.T332N and clade B tier 1 SF162 by rabbit plasma. The heat-inactivated plasma was diluted by 50-fold and subjected to a 3-fold dilution series in the TZM-bl assay. ID₅₀ NAb titers are labeled for all plots except for the time points of day -10 (-d10) and week 1 (w1), as well as week 6 (w6) for the trimer group tested against BG505.T332N. In (D) and (E), samples obtained from eight rabbits in the trimer group (34, 35, 36, and 37) and the ferritin group (62, 63, 64, and 65) at the time points of day -10 (-d10) and weeks 1, 6, 14, 22, and 30 (w1, w6, w14, w22, and w30) were analyzed in ELISA and neutralization assays. (F) Neutralization of 12 isolates in the global panel by rabbit plasma from the trimer group. (G) Neutralization of 12 isolates in the global panel by rabbit plasma from the ferritin group. In (F) and (G), samples at day -10 (-d10) and week 22 (w22) were analyzed to examine plasma neutralization of heterologous HIV-1 clones. To increase the sensitivity of detection, rabbit plasma was diluted by 20-fold followed by a 3-fold dilution series in TZM-bl assays. To reduce false positives caused by non-specific antiviral proteins present in the rabbit plasma, a simple metric was utilized that directly compares the percent neutralization of the w22 sample to that of the -d10 sample from the same animal at the 20- and 60-fold dilutions. The w22 signals at both dilutions must be 2-fold greater than the corresponding -d10 signals for a sample to be considered neutralizing a virus clone in the global panel. By this metric, the w22 samples in both trimer and ferritin groups neutralized p398F1 (clade A), p25710 (clade C), pX2278 (clade B), and pCNE8 (clade A/E) among others. ID₅₀ NAb titers are only labeled for p398F1, for which 60-80% neutralization was observed for w22 compared to -d10, approaching ID₅₀ values observed for the autologous neutralization.

Table S1. X-ray data collection and refinement statistics.

Data collection	H078.14 UFO-BG + Fab PGT124 + Fab 35O22
Beamline	APS 23-IDB
Wavelength (Å)	1.0332
Detector	Eiger 16M
Space group	P6 ₃
Unit cell parameters (Å)	
a, b, c (Å)	127.3 127.3 316.3
Resolution (Å)	50.0-4.6 (4.68-4.60) ^a
Total reflections	82,828
Unique reflections	15,619 (798)
Redundancy	5.3 (5.2) ^a
Completeness (%)	96.9 (98.0) ^a
$\langle I/\sigma_i \rangle$	7.7 (1.25) ^a
R_{sym}^b	0.29 (>1.00) ^a
R_{pim}^c	0.12 (0.76) ^a
$CC_{1/2}^d$	0.76 (0.58) ^a
Refinement statistics	
Resolution (Å)	48.8-4.6 (4.9-4.6) ^a
Reflections (work)	14,840
Reflections (test)	749
$R_{\text{cryst}}(\%)^e$	31.2
$R_{\text{free}}(\%)^f$	34.0
Average B value (Å ²) (Proteins/Glycans)	272 / 323
RMSD from ideal geometry	
Bond length (Å)	0.003
Bond angles (°)	0.678
Ramachandran statistics (%)	
Favored	93.67
Allowed	5.85
Outliers	0.48
PDB ID	6CE0

^aNumbers in parentheses are for highest resolution shell

^b $R_{\text{sym}} = \sum_{\text{hkl}} \sum_i |I_{\text{hkl},i} - \langle I_{\text{hkl}} \rangle| / \sum_{\text{hkl}} \sum_i I_{\text{hkl},i}$, where $I_{\text{hkl},i}$ is the scaled intensity of the i^{th} measurement of reflection h, k, l, and $\langle I_{\text{hkl}} \rangle$ is the average intensity for that reflection

^c $R_{\text{pim}} = \sum_{\text{hkl}} (1/(n-1))^{1/2} \sum_i |I_{\text{hkl},i} - \langle I_{\text{hkl}} \rangle| / \sum_{\text{hkl}} \sum_i I_{\text{hkl},i}$, where n is the redundancy

^d $CC_{1/2} = \text{Pearson Correlation Coefficient between two random half datasets}$

^e $R_{\text{cryst}} = \sum_{\text{hkl}} |F_o - F_c| / \sum_{\text{hkl}} |F_o| \times 100$

^f R_{free} was calculated as for R_{cryst} , but on a test set comprising 5% of the data excluded from refinement